Geol. Mag. **156** (*3*), *2019, pp. 447–470* © *Cambridge University Press 2017*
doi:10.1017/S0016756817000887

Cambro-Ordovician vs Devono-Carboniferous geodynamic evolution of the Bohemian Massif: evidence from *P–T–t* studies in the Orlica–Śnieżnik Dome, SW Poland

MIROSŁAW JASTRZĘBSKI*†, BARTOSZ BUDZYŃ‡ & WOJCIECH STAWIKOWSKI§

*Institute of Geological Sciences, Polish Academy of Sciences, Research Centre in Wrocław INGPAN, ul. Podwale 75, 50-449 Wrocław, Poland
‡Institute of Geological Sciences, Polish Academy of Sciences, Research Centre in Kraków INGPAN, ul. Senacka 1, 31-002 Kraków, Poland
§Institute of Geology, Adam Mickiewicz University, ul. Krygowskiego 12, 61-680 Poznań, Poland

(*Received* 19 December 2016; *accepted* 15 September 2017; *first published online* 16 November 2017)

Abstract – The pressure–temperature–deformation–time (*P–T–d–t*) record of metagranitic rocks and adjacent diverse rocks of the metavolcano-sedimentary group from the Orlica–Śnieżnik Dome (OSD) in SW Poland is examined. The study aims to better understand the course of the break-up of northern Gondwana and the overprinting Variscan tectonometamorphism in the NE Bohemian Massif. We test the existing hypotheses that explain the Cambro-Ordovician thermal event recorded in the meta-supracrustal group by (i) syn-deformational regional metamorphism or (ii) the contact metamorphism of the (meta)sedimentary rocks around the intruding ~490–500 Ma granitic magmas. In addition, we check the extent and timing of the Variscan prograde and retrograde medium-pressure metamorphism in the OSD. The results imply that Early Palaeozoic monazites, rarely preserved in both rock groups, document ~490–500 Ma volcanic and plutonic events related to the Gondwana's break-up and following disturbance of the Th–U–Pb system during younger, Variscan events. The monazite geochronology reveals no distinct Cambro-Ordovician thermal aureole around the post-granitic orthogneisses. However, no large-scale Variscan juxtaposition is evident between the two main OSD rock groups or within the meta-supracrustal rocks. Consistent *P–T–d–t* results for the meta-supracrustal rocks and the orthogneisses suggest that their precursors contacted before the Variscan tectonometamorphism. The directly contiguous ortho- and paragneisses together experienced tectonometamorphic processes at maximum depths that correspond to 7.5–8.0 kbar and maximum temperatures of ~600–620°C, as a result of the Variscan collision of Gondwana and Euramerica. The continental collision-related events intensified at ~360 Ma and ~330–340 Ma.

Keywords: Gondwana continent, Cambro-Ordovician thermal event, Variscan Orogen, Bohemian Massif, Orlica-Śnieżnik Dome.

1. Introduction

In orogenic systems, older structures and mineral assemblages that are related to pre- or early-orogenic thermal events can be completely obliterated by intense tectonometamorphism during subsequent orogenic processes. One of the major open questions in studies on the evolution of the Mid-European Variscan belt is to fully understand the role of the pre-Variscan, Cambro-Ordovician thermal event that preceded the structurally dominant, mainly Carboniferous tectonometamorphism. The Cambro-Ordovician event produced volumetrically significant igneous rocks that were generated during rifting at the northern margin of the Gondwana continent and the resultant opening of the Rheic Ocean after the Neoproterozoic Cadomian orogeny (e.g. Pin & Marini, 1993; Murphy *et al.* 2006; Pin *et al*. 2007; von Raumer & Stampfli, 2008; Nance *et al.* 2012). This process is considered to be polyphase and diachronous (e.g. Linnemann *et al.* 2008, 2014; Žák, Kraft & Hajná, 2013), and to be accompanied by the arc–arc collision in the eastern sectors of the Northern Gondwana (e.g. von Raumer *et al.* 2015). Moreover, heat induced by upwelling mantle and intruding voluminous granitic magmas during the Cambro-Ordovician extension could also have generated wide areas of contact and/or regional metamorphism. In the Bohemian Massif (Fig. 1a), the large Mid-European unit of the Variscan belt, (meta)igneous rocks of Cambro-Ordovician protolith ages occur together with (meta)volcano-sedimentary rocks of older or comparable protolith ages (e.g. Drost *et al.* 2004; Cháb, Stránik & Eliáš, 2007; Oberc-Dziedzic *et al.* 2010; Žák, Kraft & Hajná, 2013). Despite the strong Variscan overprint, the possibility that a (tectono)metamorphic event directly preceded the emplacement of widespread ~490–500 Ma felsic intrusions has been proposed for both the NE (e.g. Don

†Author for correspondence: mjast@interia.pl

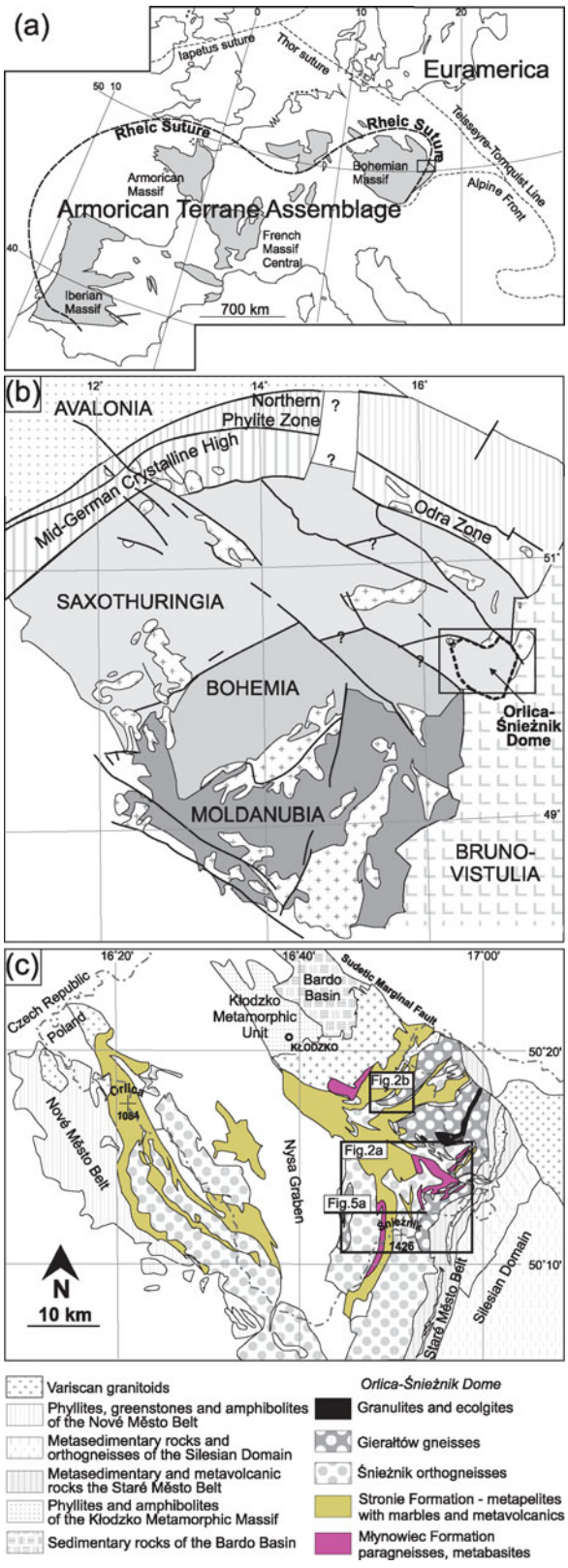

Figure 1. (Colour online) (a) Distribution of the Variscan terranes in Europe (after Linnemann *et al.* 2008). (b) Position of the Orlica–Śnieżnik Dome on a terrane map of the Bohemian Massif (modified after Franke & Żelaźniewicz, 2000). (c) Geological sketch of the Orlica–Śnieżnik Dome modified after Sawicki (1995) and Don, Skácel & Gotowała (2003), which shows the location of Figure 2a, b and the cross-section in Figure 5a.

et al. 1990; Lexa *et al.* 2005; Redlińska-Marczyńska, Żelaźniewicz & Fanning, 2016) and W part of the Bohemian Massif (Peřestý *et al.* 2017*a*, *b*).

Numerous structural and geochronological studies were conducted in the Orlica–Śnieżnik Dome (OSD) (Fig. 1b) to distinguish and reconstruct the phenomena that were related to Early and Late Palaeozoic processes. Nevertheless, major geological events in two main OSD rock groups, i.e. the orthogneisses with 490–500 Ma protolith ages and the surrounding metavolcano-sedimentary rocks, are not fully understood. One of the hypotheses that need testing postulates that ~490–500 Ma old granitic intrusions in the OSD were directly preceded by the syn-deformational, greenschist-facies metamorphism of the metavolcano-sedimentary host rocks (Don *et al.* 1990). On the other hand, the intrusive features and field evidence that signify an emplacement of the ~490–500 Ma granitic magmas (e.g. Don, 1964; Borkowska *et al.* 1990) may imply the development of a metamorphic contact aureole in the host (meta)sedimentary rocks (e.g. Teisseyre, 1961; Don, Skácel & Gotowała, 2003). Finally, in the context of the Late Palaeozoic closure of the Rheic Ocean and development of the Variscan belt, one of the most important questions refers to the extent of the subduction-related, high-pressure metamorphism, and the age of the prograde metamorphism in the studied unit. The complex Variscan evolution of the OSD produced both (ultra?)high-pressure ((U?)HP) and medium-pressure (MP) rocks (e.g. Bakun-Czubarow, 1992; Kryza, Pin & Vielzeuf, 1996; Don, Skácel & Gotowała, 2003). The orthogneisses at direct contacts with the eclogite bodies are often interpreted to have co-experienced these (U)HP metamorphic conditions (Bröcker & Klemd, 1996; Chopin *et al.* 2012*b* ; Štípská *et al.* 2012), and the OSD is only exceptionally interpreted in terms of the (U)HP unit as a whole (Gordon *et al.* 2005; Faryad & Kachlík, 2013).

This study provides new Th–U–total Pb monazite age data and pressure–temperature (*P–T*) constraints for selected rocks representing different lithological types in the OSD. The electron microprobe *in situ* dating of monazite is chosen because of the wide range of temperatures for monazite formation and the opportunity to link specific chemistries and textural settings to attribute absolute ages of specific geological processes (e.g. Williams, Jercinovic & Hetherington, 2007). Monazite crystals or at least their inner zones may provide a record of the presumed pre-Variscan thermal event in the investigated OSD rocks due to the high closure temperature (above 800–900 °C; Cherniak *et al.* 2004; Gardes *et al.* 2006). Fifteen rock samples that represent the orthogneisses and various rocks in the metavolcano-sedimentary Młynowiec–Stronie Group (MSG) were studied to determine whether Early Palaeozoic monazites, when present, are restricted to the orthogneiss/metasediment contact zone or are common and widespread components across the metavolcano-sedimentary group (Figs 1b, 2). The monazite dating study is intended

https://doi.org/10.1017/S0016756817000887 Published online by Cambridge University Press

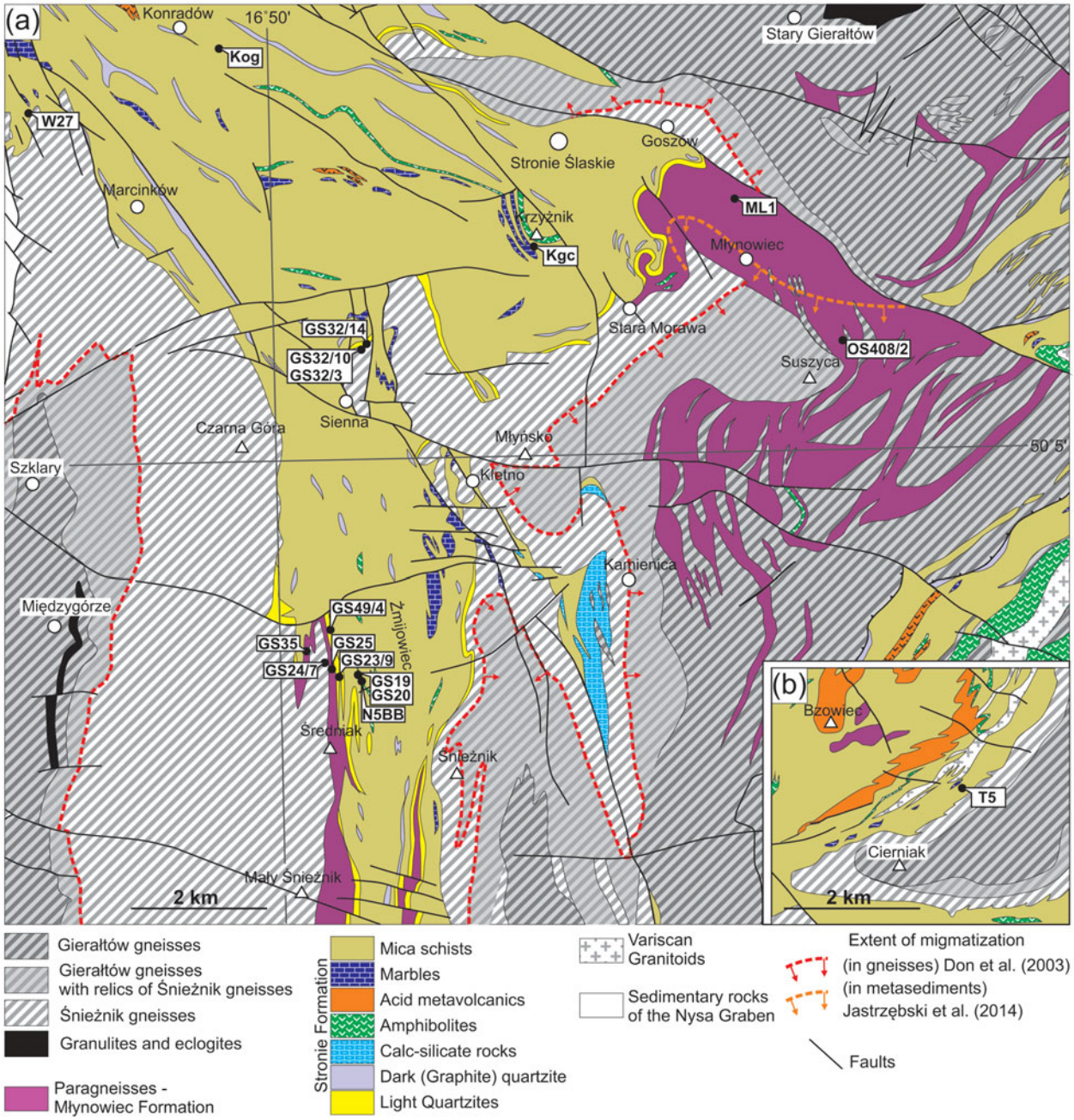

Figure 2. (Colour online) Locations of the samples analysed in this study on the geological map of the eastern area of the Orlica–Śnieżnik Dome (modified after Don, Skácel & Gotowała, 2003).

to shed new light on the unresolved discussions concerning the Cambro-Ordovician history of the OSD. The above-mentioned regularity in distribution of pre-Variscan monazites could indicate the potential existence and importance of contact metamorphic and/or regional metamorphic processes in this period. This study also attempts to establish the timing of both the dominating, penetrative metamorphic fabrics and the early metamorphic fabric, which is only occasionally preserved as mineral inclusion trails. In order to constrain the geological significance of the geochronological data, thermodynamic modelling and thermobarometric estimations are conducted for the study area, where the MSG (including paragneisses, quartzites, mica schists, acid and mafic metavolcanics) and orthogneisses are in direct contact, which is interpreted to be mainly intrusive (e.g. Don, Skácel & Gotowała, 2003). The pressure–temperature–deformation–time (*P–T–d–t*) data are correlated to unravel the significance of the interface between the metavolcano-sedimentary group and the Śnieżnik orthogneisses, and to complement the ongoing discussions on the extent of HP metamorphism in the NE part of the Bohemian Massif.

2. Geological setting and previous studies

The Orlica–Śnieżnik Dome is located in a pivotal area within the Variscan Belt. The unit is situated in the NE part of this orogen, within the suture zone between one of the elements of the

https://doi.org/10.1017/S0016756817000887 Published online by Cambridge University Press

Gondwana-derived microcontinent group (member of the Armorica Terrane Assemblage) and the Euramerica (Laurussia) continent, which is represented by the Brunovistulicum promontory (e.g. Tait *et al.* 1997; Franke, 2000; Mazur *et al.* 2006) (Fig. 1a). The OSD, considered either as a part of the Moldanubian zone (terrane) (e.g. Matte *et al.* 1990; Cymerman, Piasecki & Seston, 1997) or Saxothuringian zone (terrane) (e.g. Franke & Żelaźniewicz, 2000; Chopin *et al.* 2012*a*; Mazur *et al.* 2015) (Fig. 1b), is an internally complex unit with multiphase tectonics and strongly diversified lithology (e.g. Don *et al.* 1990) (Fig. 1c). The OSD is built by two main lithological groups of distinctly different origin. The first is the strongly variegated, meta-supracrustal Młynowiec–Stronie Group, which consists of a wide range of metasediments and minor metavolcanics. This group is subdivided into the monotonous Młynowiec Formation consisting of paragneisses and mica schists, and the Stronie Formation composed of mica schists alongside paragneisses, calcitic and dolomitic marbles, calc-silicate rocks, quartzites and graphitic schists/quartzites, and metabasaltic amphibolites and metarhyolitic leptinites (e.g. Smulikowski, 1979; Don *et al.* 1990) (Fig. 2). The mutual chronological and depositional relationships between the two originally supracrustal formations remain a topic of debate, with self-excluding conceptions of a continuous sedimentary sequence (e.g. Oberc, 1965; Smulikowski, 1979; Wojciechowska, 1993; Jastrzębski *et al.* 2010, 2014) versus two (Don *et al.* 1990; Don, Skácel & Gotowała, 2003) or three diachronous sedimentary basins (Mazur *et al.* 2012; Szczepański & Ilnicki, 2014). The deposition time of the MSG rocks has been established as Ediacaran(?) to Early Ordovician (e.g. Gunia, 1990; Jastrzębski *et al.* 2010; Mazur *et al.* 2012), with precise U–Pb zircon constraints for Late Cambrian / Early Ordovician volcanic activity registered in the Stronie Formation (~500 Ma; Murtezi & Fanning, 2005; Jastrzębski *et al.* 2015; Mazur *et al.* 2015).

The second main lithological group of the OSD was derived from igneous, plutonic precursors, and its main constituents are texturally differentiated orthogneisses, which are traditionally subdivided into two types: the Śnieżnik and Gierałtów gneisses (Fischer, 1936; Don *et al.* 1990). The Śnieżnik gneisses are represented by medium- to coarse-grained, augen and flaser gneisses, which pass into banded and laminated varieties. Some of these orthogneisses also reveal a linear rodding fabric (Żelaźniewicz, 1988; Cymerman, 1992; Lange *et al.* 2002). The second traditional variety of OSD orthogneisses, the Gierałtów gneisses, refers to finer-grained, thinly laminated rocks that pass locally into varieties with macroscopically homogeneous texture (e.g. Borkowska *et al.* 1990). The emplacement timing for the orthogneiss group protolith is the Middle Cambrian to Early Ordovician (~490–510 Ma) (e.g. Turniak, Mazur & Wysoczanski, 2000; Kröner *et al.* 2001). $\varepsilon_{Nd}500$ values between −3.3 and −5.7 suggest that the origin of the OSD gneisses is from pre-existing continental crust (Lange *et al.* 2005*b*; Buriánek *et al.* 2009). Volumetrically minor, although interpretatively significant, components of the OSD are the bodies of (U?)HP granulites and eclogites (e.g. Bakun-Czubarow, 1992, 2001; Bröcker & Klemd, 1996; Štípská *et al.* 2012), which mostly occur within the meta-igneous, orthogneissic group and reveal bimodal volcanic precursors with a minor metaplutonic origin (Bakun-Czubarow, 1998). The age of their protoliths has been constrained to the Neoproterozoic – Early Palaeozoic (Bröcker *et al.* 2010). Finally, the OSD contains and contacts with the Early Carboniferous (*c.* 340 Ma), syntectonic Variscan granitoid plutons of moderate size (e.g. Štípská, Schulmann & Kröner, 2004; Mikulski, Williams & Bagiński, 2013; Oberc-Dziedzic, Kryza & Pin, 2015).

The tectonic evolution of the OSD during the Variscan orogeny comprises three to seven deformational stages according to different authors (more review in Don *et al.* 1990; Redlińska-Marczyńska & Żelaźniewicz 2011; Skrzypek *et al.* 2011; Chopin *et al.* 2012*a* ; Żelaźniewicz *et al.* 2014), which are sometimes alternatively interpreted to be the result of continuous, progressive deformation (Cymerman, 1997). The MSG was metamorphosed under amphibolite-facies conditions (e.g. Smulikowski, 1979; Skrzypek *et al.* 2011), but the HP metamorphism of these rocks has also been suggested (e.g. Faryad & Kachlík, 2013). For the most recent review of the *P–T* estimates of the MSG see Jastrzębski, Budzyń & Stawikowski (2016). The orthogneisses are also the products of amphibolite-facies metamorphism, in part over the solidus curve; however, the orthogneisses located near the (U?)HP eclogite bodies are often interpreted to share the eclogite-facies conditions (Bröcker & Klemd, 1996; Chopin *et al.* 2012*b* ; Štípská *et al.* 2012).

Previous geochronological isotopic studies on the metamorphism of the OSD rocks involved various isotopic techniques, such as Pb–Pb zircon evaporation, the U–Pb SHRIMP (sensitive high-resolution ion microprobe) dating of zircon, the Ar–Ar and K–Ar dating of mica and amphibole, the Rb–Sr dating of micas, the Sm–Nd and Lu–Hf dating of garnet, and the Th–Pb dating of monazite (more review in Żelaźniewicz *et al.* 2014; Skrzypek *et al.* 2017). The results predominantly indicated a Late Palaeozoic metamorphic record in both the MP and volumetrically minor (U?)HP rocks, although two indistinct age groups could be distinguished. An older, Late Devonian age cluster of ~360–380 Ma was reported for the (U?)HP eclogites and granulites (Klemd & Bröcker, 1999; Gordon *et al.* 2005; Anczkiewicz *et al.* 2007). A younger, predominant Early Carboniferous age domain of 330–350 Ma was reported both for these (U?)HP rocks and granulites, and for the MP ortho- and paragneisses and mica schists (e.g. Borkowska *et al.* 1990; Brueckner, Medaris & Bakun-Czubarow, 1991; Steltenpohl *et al.* 1993; Maluski, Rajlich & Souček, 1995; Turniak, Mazur & Wysoczanski, 2000; Štípská, Schulmann & Kröner, 2004; Gordon *et al.* 2005;

https://doi.org/10.1017/S0016756817000887 Published online by Cambridge University Press

Lange, Bröcker & Armstrong, 2005*a*; Schneider *et al.* 2006; Bröcker *et al.* 2009; Jastrzębski, 2009; Walczak, 2011; Skrzypek *et al.* 2014). These authors interpreted the Late Devonian and/or Early Carboniferous dates in terms of the Variscan metamorphism of all the OSD rocks, which was accompanied by local migmatization in the orthogneisses and Młynowiec–Stronie Group and the initial exhumation of the granulites and eclogites. The (U?)HP metamorphism occurred during either the Late Devonian (375–385 Ma) (Gordon *et al.* 2005; Anczkiewicz *et al.* 2007) or the Early Carboniferous (~340–350 Ma) (Štípská, Schulmann & Kröner 2004; Bröcker *et al.* 2009; Walczak, 2011). Alternatively, isotopic U–Pb zircon dating that was interpreted in terms of the ~500 Ma migmatization of the Gierałtów gneisses could signify the occurrence of preceding, Early Palaeozoic regional metamorphism in the OSD (Żelaźniewicz *et al.* 2006; Redlińska-Marczyńska, Żelaźniewicz & Fanning, 2016).

Previous Th–U–total Pb electron microprobe dating of monazite, the method that was selected for this study, indicated the Early Carboniferous exhumation ages of the OSD granulites (Kusiak *et al.* 2008; Budzyń *et al.* 2015). Th–U–total Pb monazite records also indicated the presence of (tectono)metamorphic events at ~360 Ma and ~335 Ma in migmatic paragneisses of the Młynowiec Formation (Jastrzębski *et al.* 2014), and mica schists (Budzyń & Jastrzębski, 2015) and light quartzites of the Stronie Formation (Jastrzębski, Budzyń & Stawikowski, 2016). Integrated, the electron microprobe and isotopic methods of monazite dating indicated that ages between 360 and 340 Ma reflect the regional metamorphism, whereas the predominant age population of 330−310 Ma refers to complex retrograde processes (Skrzypek *et al.* 2017).

3. Methods of investigation

Chemical analyses of rock-forming minerals were performed using a Cameca SX 100 electron microprobe (EMP) at the Electron Microprobe Laboratory, University of Warsaw. For two samples that were dedicated to thermodynamic modelling, the whole-rock major element chemical compositions were determined by inductively coupled plasma mass spectrometry (ICP-MS) at Activation Laboratories Ltd (Actlabs, Canada). The *P–T* equilibrium assemblage diagrams for samples GS24/7 (orthogneiss) and GS25 (paragneiss) were produced using the rock composition (mol. %) reduced to an MnNCKFMASH ($MnO–Na_2O–CaO–K_2O–FeO–MgO–Al_2O_3–SiO_2–H_2O$) system. The calculations were performed using the THERMOCALC 3.33 program, which contains the thermodynamic database of Holland & Powell (1998, dataset 55). The specified *P–T* windows ranged from 400 to 700 °C and from 2 to 12 kbar. The calculations included garnet, biotite, muscovite, chlorite, chloritoid, plagioclase, K-feldspar, staurolite, silicate melt, kyanite, andalusite, sillimanite, quartz and water. The mineral chemistry analyses revealed almost pure albite domains ($An_{<3}$) in zoned plagioclases from the paragneisses and orthogneisses, so albite was added to the calculations as a pure end-member. The H_2O content was estimated to saturate all the mineral assemblages below the solidus. The activity–composition models in the thermodynamic modelling were taken from the THERMOCALC documentation page at http://www.metamorph.geo.uni-mainz.de/thermocalc/datafiles/ (MnNCKFMASH system). Additionally, an Al-in-hornblende geobarometer (Schmidt, 1992) and amphibole–plagioclase thermometer based on reaction edenite + albite = richterite + anorthite (Holland & Blundy, 1994) were applied for the amphibolite sample N5BB from the Stronie Formation. The conventional *P–T* calculations were conducted using an Excel spreadsheet developed by L. Anderson: http://www.minsocam.org/MSA/RIM/RiMG069/RiMG069_Ch04_hbld_plag_thermo-jla.xls.

The compositional wavelength-dispersive spectrometry (WDS) X-ray maps of selected monazite grains were collected using the Cameca SX 100 EMP at the Electron Microprobe Laboratory of the University of Warsaw, and the JEOL JXA-8230 SuperProbe EMP at the Laboratory of Critical Elements AGH-KGHM, Faculty of Geology, Geophysics and Environmental Protection, AGH University of Science and Technology in Kraków. The chemical analyses of monazite were performed with the Cameca SX 100 electron microprobe at the Department of Special Laboratories, Laboratory of Electron Microanalysis, Geological Institute of Dionýz Štúr (Bratislava, Slovak Republic). The analytical conditions included a 15 kV accelerating voltage, 180 nA beam current and 3 μm beam size on the carbon-coated thin sections (for more details regarding dating of monazite, the standards and counting times, see Konečný *et al.* 2004; Petrík & Konečný, 2009; Vozárová *et al.* 2014; Budzyń, Konečný & Kozub-Budzyń, 2015). The analytical results were interpreted according to the composition of the internal domains and the structural position of each monazite prior to selecting dates to calculate the weighted average ages. The concentrations of U, Th and Pb in the monazite were recalculated using the age equations from Montel *et al.* (1996) and evaluated using the in-house DAMON software (P. Konečný, unpublished) to plot histograms and isochrons. Following Williams *et al.* (2006), the term 'date' is used in this work as the number obtained from the age equation for a single spot and does not necessarily have geological significance, whereas the term 'age' is used for a result that is interpreted as providing geological significance, i.e. describing the timing of a particular event.

The mineral abbreviations after Whitney & Evans (2010) are used in this paper. The other abbreviations used include (in %) Alm (Grt) = $Fe/(Mn + Fe^{2+} + Mg + Ca) \times 100$, Grs (Grt) = $Ca/(Mn + Fe^{2+} + Mg + Ca) \times 100$, Prp (Grt) = $Mg/(Mn + Fe^{2+} + Mg + Ca) \times 100$, Sps (Grt) = $Mn/(Mn + Fe^{2+} + Mg + Ca) \times 100$, An (Pl) =

https://doi.org/10.1017/S0016756817000887 Published online by Cambridge University Press

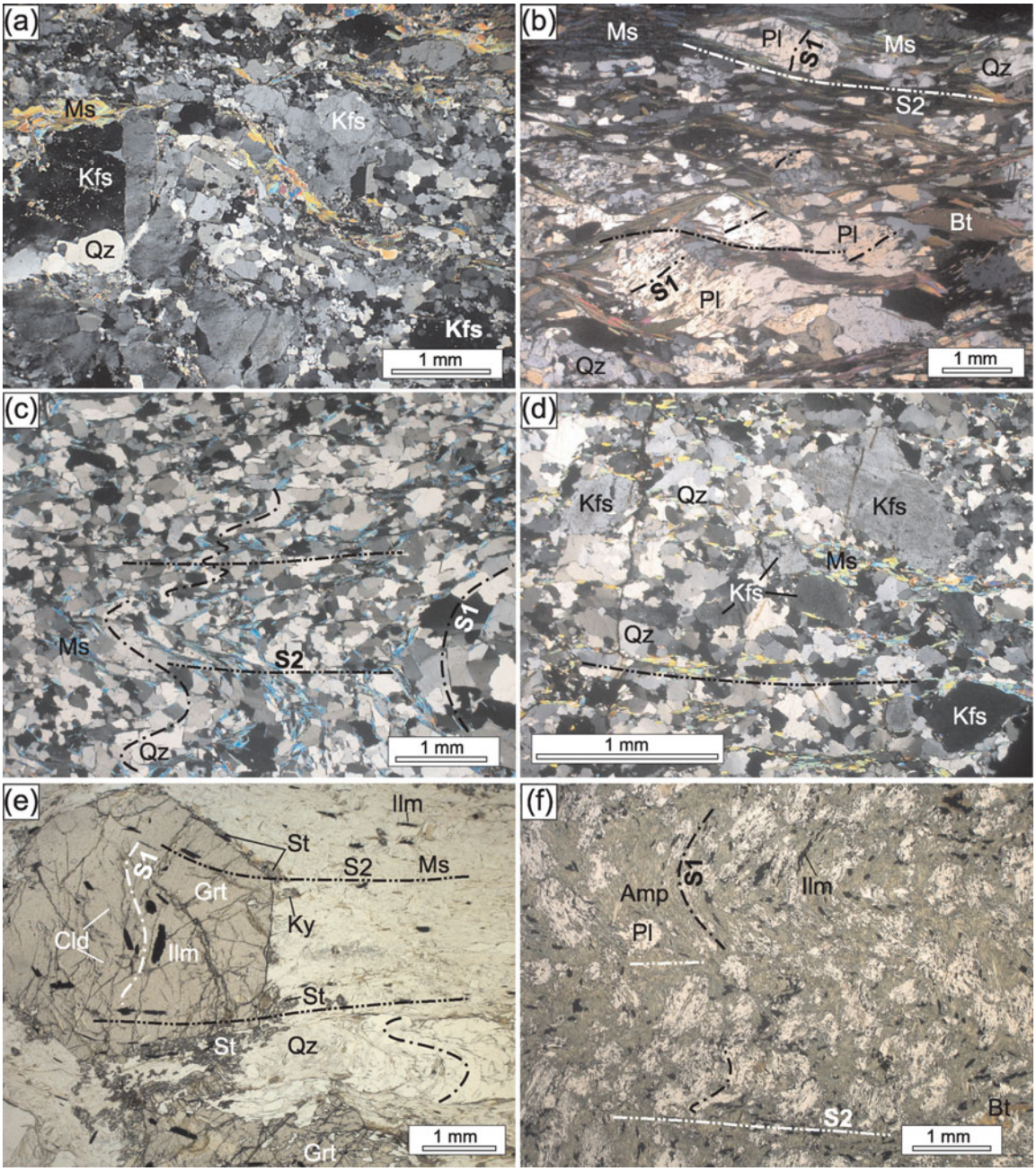

Figure 3. (Colour online) Photomicrographs showing the structures that developed in orthogneisses and metavolcano-sedimentary rocks in different areas of the Orlica–Śnieżnik Dome. (a) XPL photomicrograph showing the main foliation in the Śnieżnik orthogneisses near Mount Średniak. The gneissosity is parallel to the S2 foliation in the metasedimentary rocks and dips to the ENE at 55°. (b) XPL photomicrograph showing the S1–S2 relationships in paragneisses near Młynowiec village (sample ML1). The S1 foliation is mainly preserved in albitic cores of zoned plagioclases. The penetrative S2 foliation dips to the NE at an angle of 50°. (c) XPL photomicrograph showing the S1–S2 relationships in quartzites near Stara Morawa village. The S2 dips to the N at an angle of 25°. (d) K-feldspar-bearing quartzite near Mount Średniak (sample GS23/9). The foliation is parallel to S2 in adjacent metasediments and dips to the ENE at 60°. (e) PPL photomicrograph showing the S1–S2 relationships in mica schists near Mount Krzyżnik. The main schistosity S2 dips to the NE at an angle of 45°. (f) PPL photomicrograph showing the S1–S2 relationships in amphibolites near Mount Krzyżnik. The S2 dips to the NE at an angle of 40°.

$Ca/(Ca + Na + K) \times 100$, and XFe (Bt) = $Fe/(Fe^{2+} + Mg)$.

4. Microstructures, petrography, mineral chemistry and *P–T* evolution

The microstructural relationships in the studied mica schists, paragneisses, quartzites and amphibolites of the OSD were characterized prior to the thermodynamic modelling and application of thermobarometry. Deformational metamorphic foliations, which are termed S1–S3 in this paper, refer to those that were described in detail in a previous work (Jastrzębski *et al.* 2014). The metamorphic fabrics identified in this study are presented in Figure 3.

https://doi.org/10.1017/S0016756817000887 Published online by Cambridge University Press

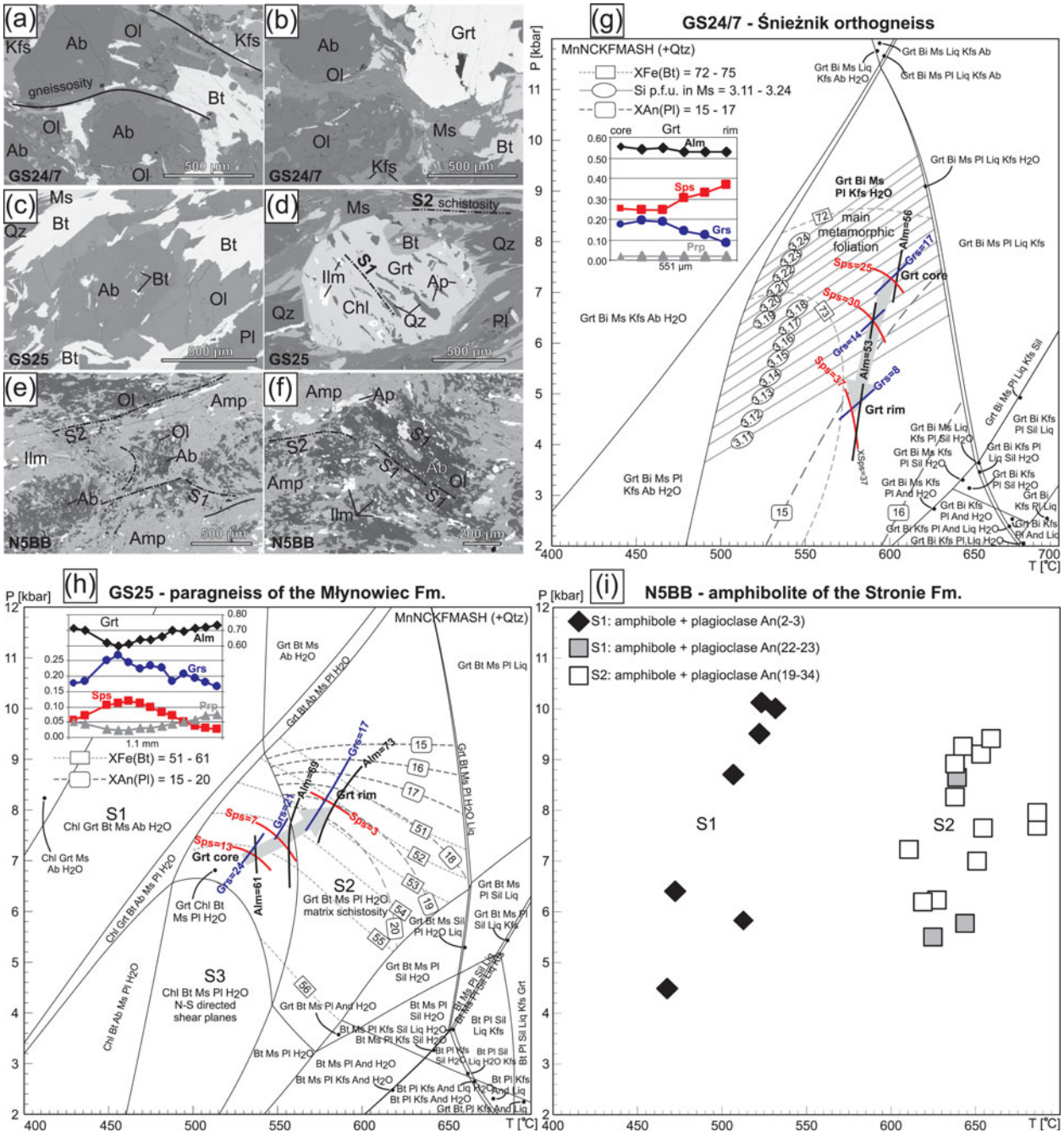

Figure 4. (Colour online) (a–f) Back-scattered electron images showing the mineral and microstructural relationships in metamorphic rocks from the Średniak area in the SE region of the Orlica–Śnieżnik Dome: (a, b) Śnieżnik orthogneiss, (c, d) paragneiss from the Młynowiec Formation, and (e, f) amphibolite from the Stronie Formation. (g) Mineral chemistry and *P–T* equilibrium assemblage diagram for the sample GS24/7. The calculated compositional isopleths of Pl, Ms and Bt reflect the measured chemical composition of the minerals that define the main gneissosity. The grey arrow refers to compositional zoning from the garnet's core to the rim. (h) Mineral chemistry *P–T* equilibrium assemblage diagram for the sample GS25. The calculated compositional isopleths of Pl and Bt reflect the measured chemical composition of the minerals that define the S2 foliation. The grey arrow refers to zonation from the garnet's core to the rim. (i) Geothermobarometry results for the sample N5BB. The squares refer to the intersection of the Al-in-amphibole barometry and the Amp–Pl thermometry results for the respective Amp–Pl pairs.

For the *P–T* reconstructions, we focused on the area between the Żmijowiec and Średniak Mountains, where the key geological boundaries of the OSD, i.e., the Śnieżnik orthogneisses/MSG paragneisses, MSG paragneisses/MSG quartzites, and MSG quartzites/MSG mica schists contacts, are exposed (Figs 4, 5). Previously, Štipská *et al.* (2012) revealed that the maximum pressures recorded by the eclogites from Międzygórze relatively close to this location (~2 km) were 15 kbar higher than those of the mica schists from Mount Żmijowiec. This suggests a significant metamorphic and tectonic discontinuity (see Fig. 5a). Our study constrains the relationships of the structures and metamorphism in this area, with special attention on the *P–T* reconstructions of the Śnieżnik orthogneisses, paragneisses in the Młynowiec Forma-

https://doi.org/10.1017/S0016756817000887 Published online by Cambridge University Press

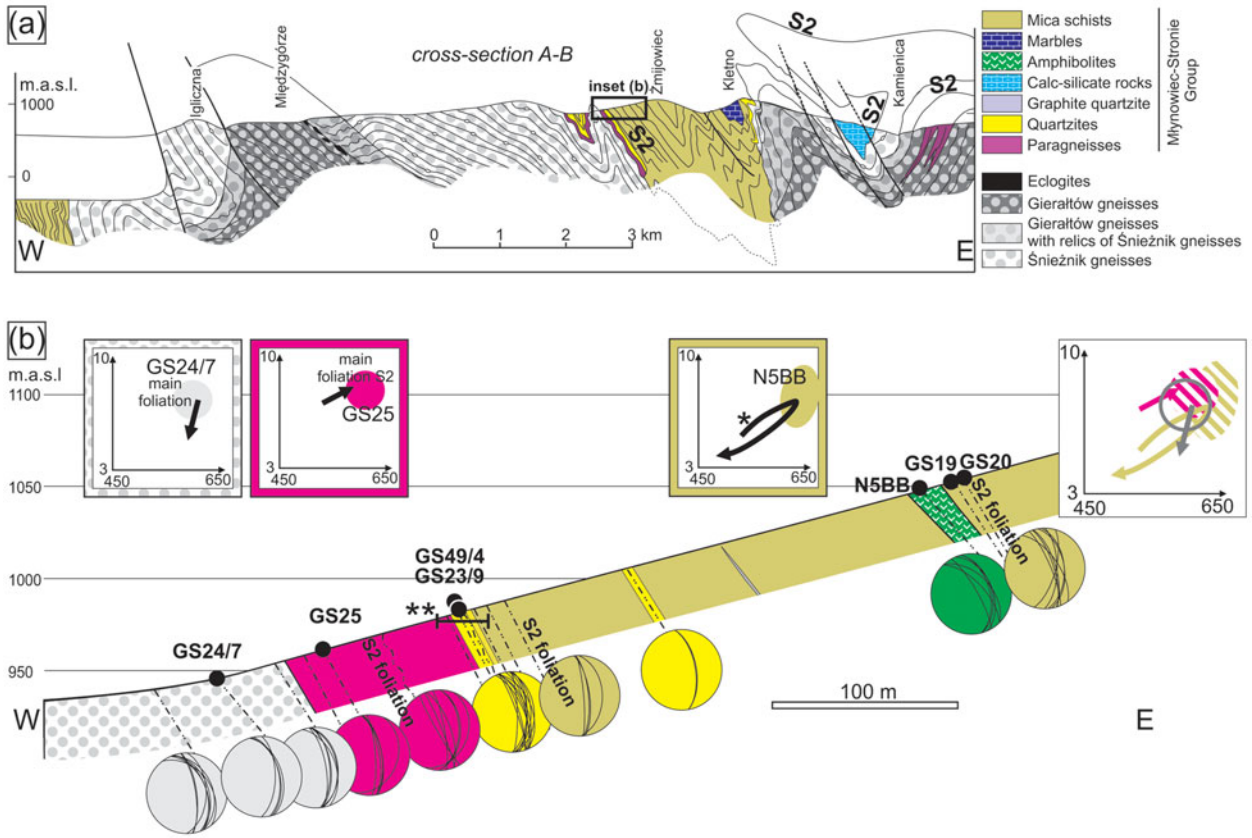

Figure 5. (Colour online) (a) Geological cross-section through the SE area of the Orlica–Śnieżnik Dome (modified after Don, 1982). The different orientation of the penetrative foliation S2 subparallel to the lithological contacts in metasedimentary rocks is highlighted. The location of the cross-section is shown in Figure 1b. (b) Geological cross-section through the Średniak area. The *P–T* data obtained in this study and the *P–T* path determined by Štipská *et al.* (2012), the latter indicated by (*) in the referred section of the Średniak area. Details of the boundary rock sequence between the Młynowiec and the Stronie Formation. indicated by (**) in the profile are presented in Jastrzębski *et al.* (2014).

tion and amphibolites in the Stronie Formation cropping out in the Żmijowiec/Średniak area, to determine whether and how these rocks differed in their *P–T* evolution.

The structural observations in the Średniak–Żmijowiec area showed that the penetrative foliation in the orthogneisses, MSG paragneisses, mica schists, mica- and K-feldspar-quartzites, and amphibolites had similar orientation, dipping to the ENE at moderate to high angles (Fig. 5b). The meta-supracrustal rocks sometimes contained relics of the earlier metamorphic fabric visible in rock exposures, and preserved at the micro-scale as inclusion trails in plagioclase or garnet porphyroblasts. The thermobarometric calculations constrained the *P-T* conditions of these metamorphic foliations.

4.a. Śnieżnik orthogneiss – sample GS24/7

Sample GS24/7 is a medium-grained, garnet-bearing orthogneiss, which was collected ~50 m west of the contact between metaigneous rocks and the Młynowiec–Stronie Group. Its macrotextural features (small augen, distinct quartzose and feldspathic domains, stretching lineation) indicate that this sample belongs to the Śnieżnik gneisses in the OSD metagranitoids. The chemical composition of this sample (in wt %) is $SiO_2 = 74.83$, $Al_2O_3 = 13.07$, $Fe_2O_3(T) = 1.92$, $MnO = 0.05$, $MgO = 0.36$, $CaO = 0.79$, $Na_2O = 2.9$, $K_2O = 4.9$, $TiO_2 = 0.19$, $P_2O_5 = 0.15$, and LOI = 0.55. It is composed of plagioclase, K-feldspar, quartz, muscovite, biotite and accessory garnet. Two distinct compositional zones can be distinguished in the plagioclases. The cores of plagioclases often consist of inclusion-free albite ~1 mm in diameter and are overgrown by oligoclase rims (An = 15–17) up to 300 μm thick. These rims are often elongated parallel to the gneissosity (Fig. 4a, b). Other minerals that define the main foliation include quartz, muscovite (3.11–3.24 Si p.f.u.), and biotite ($X_{Fe} = 72–75$). This metamorphic foliation is generally parallel to the S2 foliation in the adjacent metavolcano-sedimentary rocks of the MSG (Fig. 5b). Irregularly shaped garnet up to 1 mm in diameter is a minor constituent of this rock. The compositional zoning in the garnet shows decreasing Fe (Alm from 56 to 53) and Ca (Grs from 17 to 8) and increasing Mn (Sps from 25 to 37) from core to rim. The Mg values are constant and very low (Prp at 2) (Fig. 5b; Table 1).

https://doi.org/10.1017/S0016756817000887 Published online by Cambridge University Press

Table 1. Representative mineral analyses of samples GS24/7, GS25 and N5BB

Rock	GS24/7 – orthogneiss						GS25 – paragneiss							N5BB – amphibolite				
Mineral	Pl	Pl	Bt	Ms	Grt	Grt	Pl	Pl	Chl	Bt	Ms	Grt	Grt	Pl	Pl	Amp	Pl	Amp
Number	#pl5	#pl7	#bt3	#ms2	#grt1	#grt6	#ab1	#pl11	#chl3	#bt14	#ms3	#grt7	#grt15	#pl9	#pl10	#amp9	#am14	#am11
Position	Pl core	Pl rim || S2	matrix || S2	matrix || S2	Grt core	Grt rim	Pl core	S2, Pl rim	S1,incl. in Grt	matrix S2	matrix S2	Grt core	Grt rim	S1, Pl core	S1, Pl rim	S1,incl. in Ab	matrix S2	matrix S2
SiO_2	69.20	64.89	35.84	48.47	37.03	36.73	68.38	63.98	24.42	35.46	46.48	37.29	36.98	67.91	62.74	45.75	63.16	46.12
TiO_2	n.a.	n.a.	2.50	0.49	0.06	0.18	0.00	0.00	0.14	1.09	0.36	0.18	0.02	n.a.	n.a.	0.35	n.a.	0.33
Al_2O_3	19.43	22.14	18.07	30.44	20.50	20.38	19.95	22.81	23.06	18.58	35.70	20.52	20.56	20.39	23.52	11.57	23.42	10.76
Fe_2O_3	n.a.	n.a.	n.a.	n.a.	0.63	0.52	0.00	n.a.	n.a.	n.a.	n.a.	0.00	0.00	n.a.	n.a.	n.a.	n.a.	n.a
FeO	0.00	0.00	24.34	4.02	24.67	23.37	0.04	0.01	26.31	20.83	1.66	1.12	0.81	0.11	0.16	14.61	0.12	15.96
MnO	n.a.	n.a.	0.56	0.12	10.85	16.01	0.00	n.a.	0.23	0.11	0.00	27.97	32.81	n.a.	n.a.	0.33	n.a.	0.31
MgO	n.a.	n.a.	5.14	1.52	0.48	0.49	0.00	n.a.	14.26	9.69	0.68	5.33	1.26	n.a.	n.a.	12.18	n.a.	12.12
CaO	0.03	3.37	0.00	0.00	6.01	2.82	0.62	3.94	0.02	0.00	0.00	0.65	1.85	0.44	4.59	10.21	4.28	9.75
Na_2O	11.68	9.64	0.08	0.28	0.00	0.02	10.86	8.89	0.00	0.15	2.02	8.66	5.88	11.39	8.98	1.72	9.04	1.48
K_2O	0.18	0.12	9.72	11.20	0.00	0.00	0.06	0.12	0.01	9.24	8.53	0.03	0.00	0.04	0.05	0.31	0.03	0.28
Total	100.52	100.16	96.25	96.54	100.23	100.52	99.91	99.75	88.45	95.15	95.43	101.75	100.17	100.28	100.04	97.03	100.05	97.10
Oxygens	8	8	11	11	12	12	8	8	28	11	11	12	12	8	8	23	8	23
Si	3.005	2.853	2.773	3.237	3.001	2.994	2.984	2.824	5.129	2.720	3.072	2.972	2.982	2.961	2.775	6.748	2.789	6.822
Ti	0.000	0.000	0.145	0.025	0.004	0.011	0.000	0.000	0.022	0.063	0.018	0.011	0.001	—	—	0.039	—	0.036
Al	0.995	1.148	1.648	2.396	1.958	1.958	1.026	1.187	5.710	1.680	2.782	1.928	1.954	1.048	1.226	2.011	1.219	1.875
Fe^{3+}	—	—	—	—	0.038	0.032	—	—	—	—	—	0.000	0.000	—	—	0.000	—	0.000
Fe^{2+}	0.000	0.000	1.575	0.225	1.672	1.593	0.001	0.000	4.622	1.336	0.092	0.067	0.049	0.004	0.006	1.802	0.004	1.975
Mn	—	—	0.037	0.007	0.745	1.105	—	—	0.041	0.007	0.000	1.864	2.212	—	—	0.041	—	0.039
Mg	—	—	0.593	0.151	0.058	0.060	—	—	4.464	1.108	0.067	0.360	0.086	—	—	2.678	—	2.673
Ca	0.001	0.159	0.000	0.000	0.522	0.246	0.029	0.186	0.005	0.000	0.000	0.077	0.222	0.020	0.217	1.613	0.202	1.546
Na	0.983	0.822	0.012	0.036	0.000	0.003	0.919	0.761	0.000	0.022	0.259	0.739	0.508	0.963	0.770	0.492	0.774	0.424
K	0.010	0.007	0.960	0.954	0.000	0.000	0.003	0.007	0.003	0.904	0.719	0.005	0.000	0.002	0.003	0.058	0.002	0.052
Total	4.994	4.988	7.743	7.031	7.997	8.002	4.964	4.966	19.995	7.840	7.008	8.022	8.015	4.998	4.997	15.482	4.990	15.442
XFe			73	60	97	96			51	55	58	96	91			40		42
Grs					17	8						24	17					
Sps					25	37						12	3					
Alm					56	53						61	73					
Prp					2	2						3	7					
An	0	16					3	20						2	22		21	

Note: n.a. - not analysed.

The calculations of the mineral stability fields indicated that the mineral assemblage Bt–Ms–Pl–Kfs + Grt was stable over a wide *P–T* sector (Fig. 4g). Albite cores of plagioclase blasts may represent earlier, greenschist-facies metamorphic conditions, but a magmatic origin for these inclusion-free grains is also possible. More accurate *P–T* estimates for the development of the main metamorphic foliation in the studied Śnieżnik orthogneiss can be deduced from the compositional isopleths of the minerals that define this structure. As evidenced by the anorthite content in the plagioclase, Si p.f.u. in the muscovite and XFe in the biotite, the main foliation developed at temperatures of ~600 °C and under medium pressure conditions. Muscovite and biotite isopleths indicated pressure conditions that did not exceed 9 kbar (Fig. 4g). The structural position of the garnet is not clear (Fig. 4b). The intersections of the almandine, spessartine and grossular isopleths indicate, however, the retrogressive portion of the *P–T* path from 7.5 kbar and 600 °C to 4.5 kbar and 580 °C. Cooling of 20 °C during the ~10 km uplift suggests a relatively high exhumation rate. The *P–T* estimations for the Grt rim were outside the lowest Si-in muscovite isopleths, so this uplift at least partially may have occurred after the main gneissosity was established.

4.b. Młynowiec Formation – sample GS25 (paragneiss)

The sample GS25 is a fine-grained garnet-bearing paragneiss that consists of plagioclase, quartz, biotite and garnet, with sporadic chlorite, muscovite and tourmaline blasts. The chemical composition of this sample (in wt %) is $SiO_2 = 57.04$, $Al_2O_3 = 20.65$, $Fe_2O_3(T) = 6.17$, $MnO = 0.04$, $MgO = 2.44$, $CaO = 0.76$, $Na_2O = 2.12$, $K_2O = 5.29$, $TiO_2 = 0.77$, $P_2O_5 = 0.26$, and $LOI = 2.62$. The sample GS25 represents the Młynowiec Formation (lower unit of the MSG) that contacts the Śnieżnik orthogneisses near Mount Średniak (Figs 2a, 5b). The outcrop is located ~25–30 m from the contact between the Młynowiec Formation and the orthogneisses. Plagioclase porphyroblasts (up to 1.3 mm) are zoned (Fig. 4c; Table 1), with purely albitic cores and oligoclase (An = 15–20) in the rims. Garnet blasts that are ~1 mm in diameter contain S1 inclusion trails of quartz, chlorite, muscovite, apatite and ilmenite (Fig. 4d; Table 1) that are oblique to the external main foliation S2. The garnet grains reveal growth zoning from core to rim, i.e. decreasing Mn (Sps from 13 to 3) and Ca (Grs from 24 to 17) with increasing Mg (Prp from 3 to 7) and Fe (Alm from 61 to 73). The main foliation is defined by the parallel alignment of muscovite, biotite and quartz. The biotites in the S2 matrix foliation yielded XFe = 51–61. The retrogressive shear planes S3 in the paragneiss consist of chlorite, muscovite and biotite and developed sub-parallel to the S2 foliation.

The stability fields of the mineral assemblages that define the S1 (Chl–Bt–Ab–Ms–Grt–Qz), S2 (Bt–Grt–Ms–Pl–Qz) and S3 foliations (Chl–Ms–Bt–Pl–Qz) suggest a clockwise *P–T* path. The mineral assemblage that forms the main foliation (S2) in the studied paragneiss was stable under temperatures from 520 to 650 °C and pressures up to 12 kbar. The isopleth thermobarometry of sample GS25 provided more specific *P–T* conditions of the transition from the S1 to S2 foliation. According to the calculations, albite growth was terminated and oligoclase growth begun at *P–T* conditions that are defined by the relatively narrow stability field of Chl–Grt–Bt–Ab–Pl (Fig. 4h). The positions of intersecting compositional isopleths of Grs, Alm and Sps tightly constrain the *P–T* conditions of this event, indicating an increase in temperature from 500 to 580 °C and pressure from 7.0 to 8.4 kbar. The intersections of compositional isopleths of biotite (XFe) and plagioclase (An) are consistent with the conditions that were calculated for the garnet rim compositions.

4.c. Stronie Formation – sample N5BB (amphibolite)

Sample N5BB is a fine- to medium-grained amphibolite that consists of alternating, discontinuous laminae that are richer in either plagioclase or amphibole and displays compositional banding. The irregularly shaped plagioclase blasts have variable sizes from 0.1 to 1.2 mm in diameter. These grains include almost purely albitic cores (An = 2–3) surrounded by thicker, homogeneous, Ca-richer rims with anorthite content of 15–17 (Fig. 4). The plagioclase blasts (both their albite cores and oligoclase rims) often contain indistinct relics of S1 foliation, which are preserved as elongated amphibole, ilmenite, epidote and apatite blasts. The S1 foliation is usually oriented obliquely to the penetrative foliation S2. The latter mainly consists of plagioclase, amphibole and ilmenite, with some epidote and chloritized biotite blasts. The amphiboles are mostly subhedral and form elongated grains up to 1 mm long. The amphibole inclusions in the albites and amphiboles that form the main penetrative foliation exhibit similar compositions, falling between Mg-hornblende and tschermakite with XMg ranging from 0.56 to 0.66 (Table 1).

Conventional thermobarometry calculations for the sample N5BB were conducted to constrain the *P–T* conditions of the development of the S1 and S2 mineral assemblages in the amphibolites from the Stronie Formation in the Średniak–Żmijowiec area. The amphibole blasts of the S1 foliation are present in both the albite cores and oligoclase rims. Calculations performed for seven albite–amphibole (inclusions in albite) pairs revealed temperatures of 350–470 °C. The Al-in-hornblende barometry used for these amphiboles yielded a relatively wide range of pressures from 4.5 to 10.1 (black squares in Fig. 4i). Thermobarometry applied to three pairs of amphiboles in oligoclase rims produced temperatures of 625–640 °C and pressures of 5.5–8.6 kbar. The temperature estimations for 12 oligoclase–amphibole pairs

https://doi.org/10.1017/S0016756817000887 Published online by Cambridge University Press

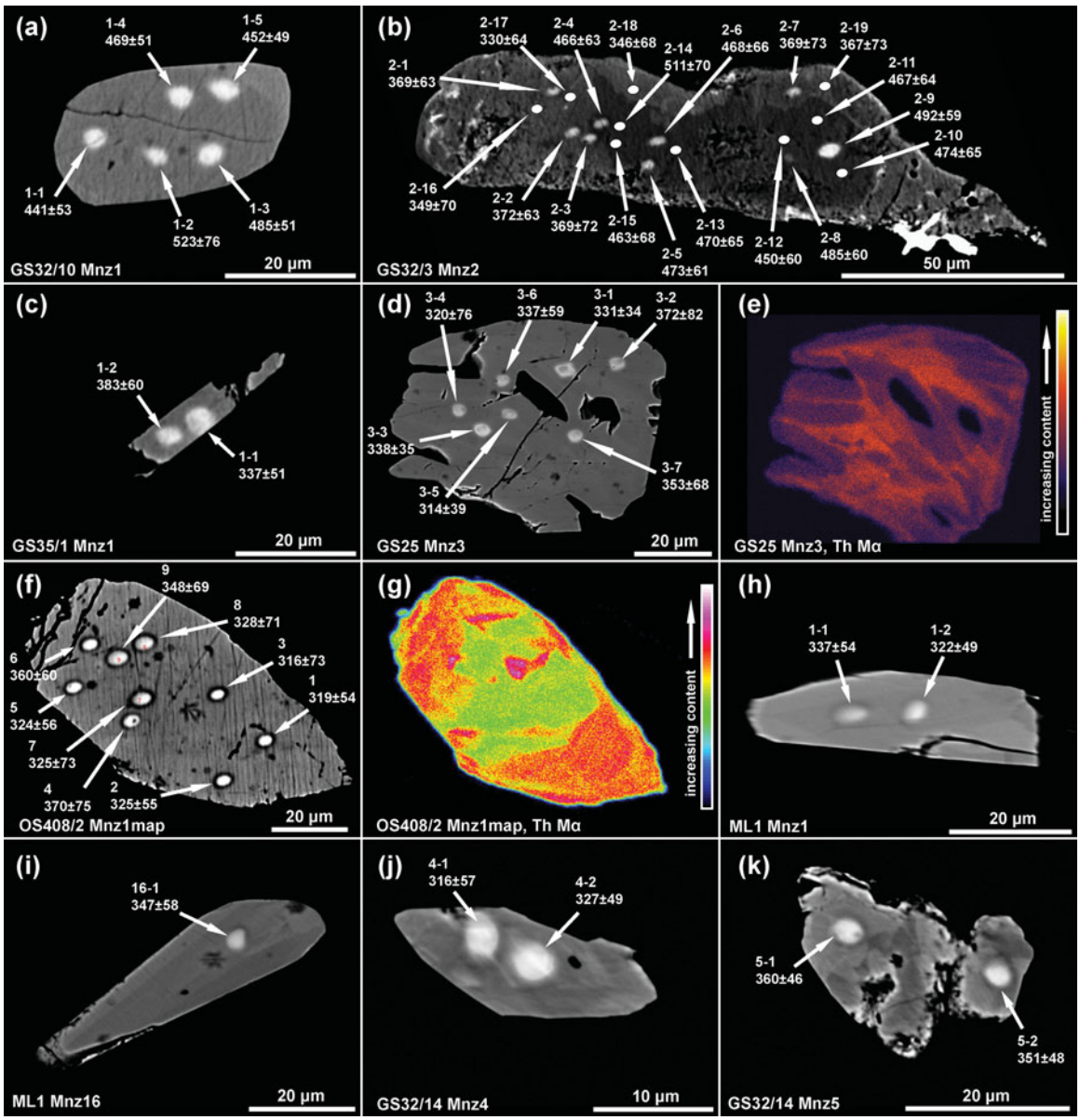

Figure 6. (Colour online) BSE images and WDS X-ray maps of representative monazite grains for geochronology. The spot labels correspond to the data in Appendix II; the Th–U–total Pb dates are listed with 2σ errors (95 % confidence level).

that were related to the formation of the S2 foliation ranged from 610 to 680 °C. The calculated pressures for these amphiboles fell between 6.2 and 9.2 kbar. The intersections between the thermometry and barometry are shown in Figure 4i and Table 1. The input data for the calculations in Figure 4i are presented in Appendix I.

5. Monazite geochronology

5.a. Orthogneisses

The monazite in the Śnieżnik orthogneiss GS32/10 comprises 15–35 μm anhedral to subhedral grains (Fig. 6a), which are present in matrix and accompanied by quartz and muscovite. The monazite grains are either homogeneous or, more rarely, show distinct core–rim relations. The EMP dating revealed a broad spectrum of dates from 311 to 523 Ma, without a specific age cluster (Fig. 7a). Dates falling into the time span 439–523 Ma were recognized in 30–35 μm grains, while smaller grains showed a record of 311–395 Ma. The similar compositional variation in the monazite across all the dates prevents this monazite growth from being linked with the evolution of other minerals (Table 2).

The monazite in the Śnieżnik orthogneiss GS32/3 comprises anhedral, 5 × 10 μm to 50 × 150 μm grains in matrix or as inclusions in quartz, muscovite or K-feldspar. The larger monazite grains show distinct cores and rims (Fig. 6b). The very low concentrations of Th and U in the small monazite grains prevented the use of Th–U–total Pb dating. Only three matrix grains provided 22 accurate analyses (with respect to composition of monazite and totals of analyses), yielding dates from 330 to 511 Ma (Fig. 7b). The core and

https://doi.org/10.1017/S0016756817000887 Published online by Cambridge University Press

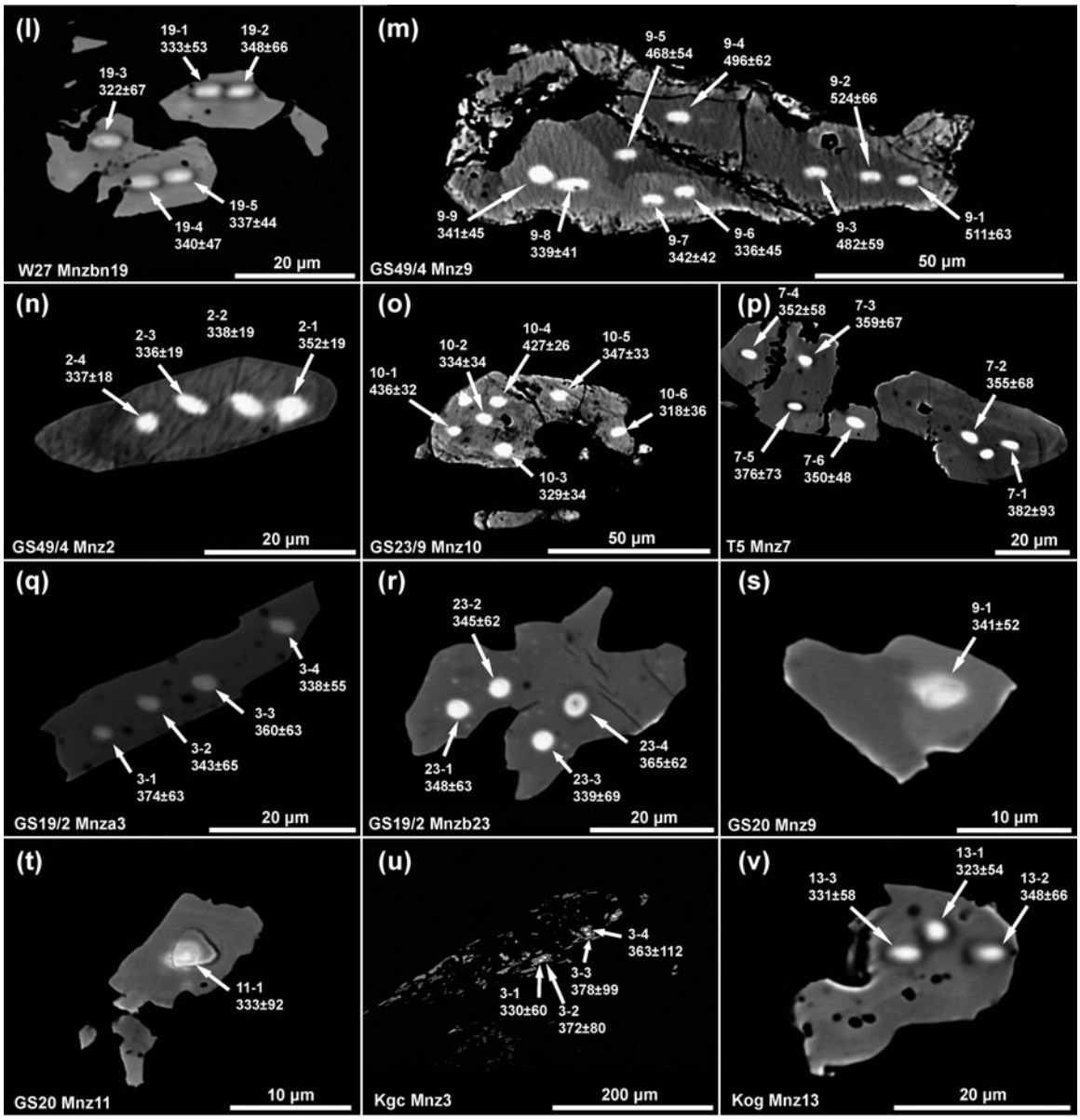

Figure 6. Continued.

rim of the grain Mnz2 yielded dates falling into the time span 450–511 Ma ($n = 11$) with distinct maxima at *c*. 470 Ma and 330–372 Ma ($n = 8$), respectively (Fig. 6b). The older population is characterized by higher Y contents than the younger monazites, i.e. ~2.79 and ~0.66 wt % Y_2O_3, respectively.

5.b. Młynowiec Formation

In the paragneiss GS35/1, subhedral to anhedral grains of monazite <20 µm across (Fig. 6c) are present in the matrix and occasionally as inclusions in muscovite. Sixteen analyses of ten grains provided dates from 304 to 384 Ma without a distinct age (Fig. 7c). Similar compositional variations in the monazite across all the dates prevent us from associating monazite growth with the evolution of other minerals.

All the selected monazite grains in the garnet-bearing paragneiss GS25 were found in the S2 matrix foliation (Figs 2a, 5b), where they form anhedral, occasionally euhedral, matrix grains from 20 to 180 µm across. The grains are mostly heterogeneous in high-contrast BSE imaging, with weak oscillatory or patchy zoning (Fig. 6d, e). Two thin sections of the paragneiss (GS25a and GS25b) were prepared for geochronology. Forty-two analyses of 7 grains in section GS25a and 81 analyses of 28 grains in section GS25b yielded dates from 295 to 399 Ma, with a predominant spectrum of 330–340 Ma. Despite the lack of textural evidence, the bimodal nature of the histogram suggests a record of at least two distinct events at ~360 Ma and 330–340 Ma. The weighted average age calculated from all the data is 343 ± 2.5 Ma (2σ, $n = 123$, MSWD = 1.54; Fig. 7d). No correlation exists between the Y concentration in monazite and the dates that may define the relative order of growth with respect to garnet across the determined range of 295–399 Ma (supplementary Fig. S1b in Appendix III).

https://doi.org/10.1017/S0016756817000887 Published online by Cambridge University Press

Table 2. Petrographic characteristics of the samples used in the monazite geochronological study. ŚO – Śnieżnik orthogneisses, MSG – rocks of the Młynowiec–Stronie Group

Distance from ŚO/ MSG boundary		Sample	Rock	Major minerals	Structural description	Monazite data; ages are given with 2σ errors
Śnieżnik orthogneisses (ŚO)	10 m	GS32/3	Leucocratic orthogneiss	Qz, Kfs, Ms, Pl	The gneissosity, which is mainly defined by the parallel orientation of Ms laminae, is parallel to the S2 foliation in the adjacent mica schists, paragneisses, quartzites and amphibolites.	450–511 Ma ($n = 11$), and 330–372 Ma ($n = 8$)
	2.5 m	GS32/10	Orthogneiss	Qz, Kfs, Ms, Pl	The parallel alignment of Qz, Kfs, Pl and Ms forms the main metamorphic foliation, which is oriented analogously to the S2 foliation in the rocks from the MSG in the adjacent outcrops.	439–523 Ma ($n = 8$), 311–395 ($n = 11$)
Młynowiec–Stronie Group (MSG)	5 cm	GS32/14	Pure quartzite	Qz > Ms	The main foliation is parallel to the gneissosity of the Śnieżnik orthogneisses from one side and parallel to the S2 schistosity in the mica schists from the other.	361 ± 7 Ma (MSWD 0.98, $n = 11$), 326 ± 13 Ma, MSWD 0.24 ($n = 4$)
	~15 m	W27	Grt-mica schist	Qz, Grt, Pl, Bt > Ms, Ilm	The S1 foliation is preserved in Grt blasts as inclusions of Qz and Ilm. The S2 foliation (intensely crenulated) is defined by ~1 mm Qz laminae that alternate with narrower Bt–Ms laminae.	340 ± 4 Ma (MSWD 0.64, $n = 48$)
	~25 m	GS25	Grt-paragneiss	Pl, Qz, Grt, Bt > Chl, Ms, Tur	Grt blasts (~1 mm in diameter) contain S1 inclusion trails of Qz, Chl, Ms, Ap and Ilm that are oblique to the external main foliation S2.	344 ± 3 Ma (MSWD 1.54, $n = 123$)
	~25 m	GS35/1	Paragneiss	Pl, Qz, Bt> Chl, Ms, Tur	S1 (Qz and Ilm) is included in the Pl blasts, and the S1 foliation is oriented obliquely to the external, main foliation S2.	304–384 ($n = 16$)
	~90 m	GS23/9	Kfs-quartzite	Qz, Kfs (~19 vol%), Ms, Pyr, Ap	The main foliation is parallel to the S2 schistosity in the adjacent mica schists.	454–555 Ma ($n = 5$), and 341 ± 4 Ma (MSWD 2.69, $n = 28$)
	~90 m	GS49/4	Kfs-quartzite	Qz, Kfs (~13 vol%), Ms, Pyr	The sample comes from the exposure that represents a transition from K-feldspar quartzites to pure quartzites and mica schists. The main, grain-shaped foliation is parallel to the S2 schistosity in the mica schists.	488 ± 7 Ma (MSWD 2.69, $n = 9$), 344 ± 3 Ma (MSWD 4.00, $n = 23$)
	~200 m	OS408/2	Paragneiss	Pl, Qz, Ms, Bt	The metamorphic foliation is defined by elongated Pl and Qz blasts, which are accompanied by Ms and Bt flakes.	331 ± 4 Ma (MSWD 1.05, $n = 52$)
	~200 m	T5	Grt-mica schist	Qz, Ms, Grt, Bt, Chl, Pl, Tur	This sample is a strongly mylonitic mica schist that consists of 'fish-like' Ms, Qz and rounded Grt grains (~3 mm in diameter). The mylonitic foliation S3‖S2 also contains chloritized Bt, Tur and rare ~1 mm Pl blasts.	348 ± 5 Ma (MSWD 1.02, $n = 29$)
	~300 m	GS19	Grt-mica schist	Qz, Grt, Bt, Ms, St, Ap, Cld, Ilm	Large, up to 8 mm Grt contains inclusions of Cld, Qz, Ms, Ap and Ilm that form S1 foliation. The external, penetrative S2 schistosity is defined by the parallel alignment of Bt, Ms, Qz and 200–700 μm St blasts.	345 ± 4 Ma (MSWD 1.37, $n = 80$)
	~300 m	GS20	Grt-mica schist	Qz, Grt, Bt, Ms, St, Tur, Ilm	The S1 foliation is preserved in cores of up to 6 mm Grt as inclusions of Qz and Ilm that are oriented obliquely with respect to the matrix schistosity S2. The external S2 is defined by 1 mm across laminae that are rich in Qz and alternate with laminae that consist of fine-grained Bt, Ms, St and Tur.	349 ± 5 Ma (MSWD 2.24, $n = 28$)
	~300 m	ML1	Paragneiss	Pl, Qz, Bt, Ms > Ilm, Chl, Tur	This sample contains porphyroblastic Pl with relics of older S1 foliation, which are defined by Qz, Ilm and Bt inclusions. The penetrative S2 is defined by Pl, Qz, Bt, Ms with Ilm, Chl and Tur.	340 ± 6 Ma (MSWD 1.48, $n = 21$)
	~1.5 km	Kgc	Grt-mica schist	Qz, Ms, Grt > Ilm, St, Bt, Chl, Cld, Tur	S1 foliation is preserved in Grt cores as inclusion trails of Chl, Cld, Qz, Ilm and Rt that are oriented obliquely with respect to the matrix S2 foliation, which is defined by alternating laminae of Qz and phyllosilicates.	371 ± 8 Ma (MSWD 1.67, $n = 21$)
	>3 km	Ko	Grt-mica schist	Qz, Ms, Grt, Bt, Chl, St, Tur, Ilm, Ap	Euhedral Grt with sizes of 0.5–2.5 mm includes Qz, Ilm, Chl and Ap that form inclusion trails that are curved toward the Grt rims. The schistosity S2 is defined by alternating laminae of Qz, Ms, Bt, St and Ilm.	338 ± 5 Ma (MSWD 1.93, $n = 34$)

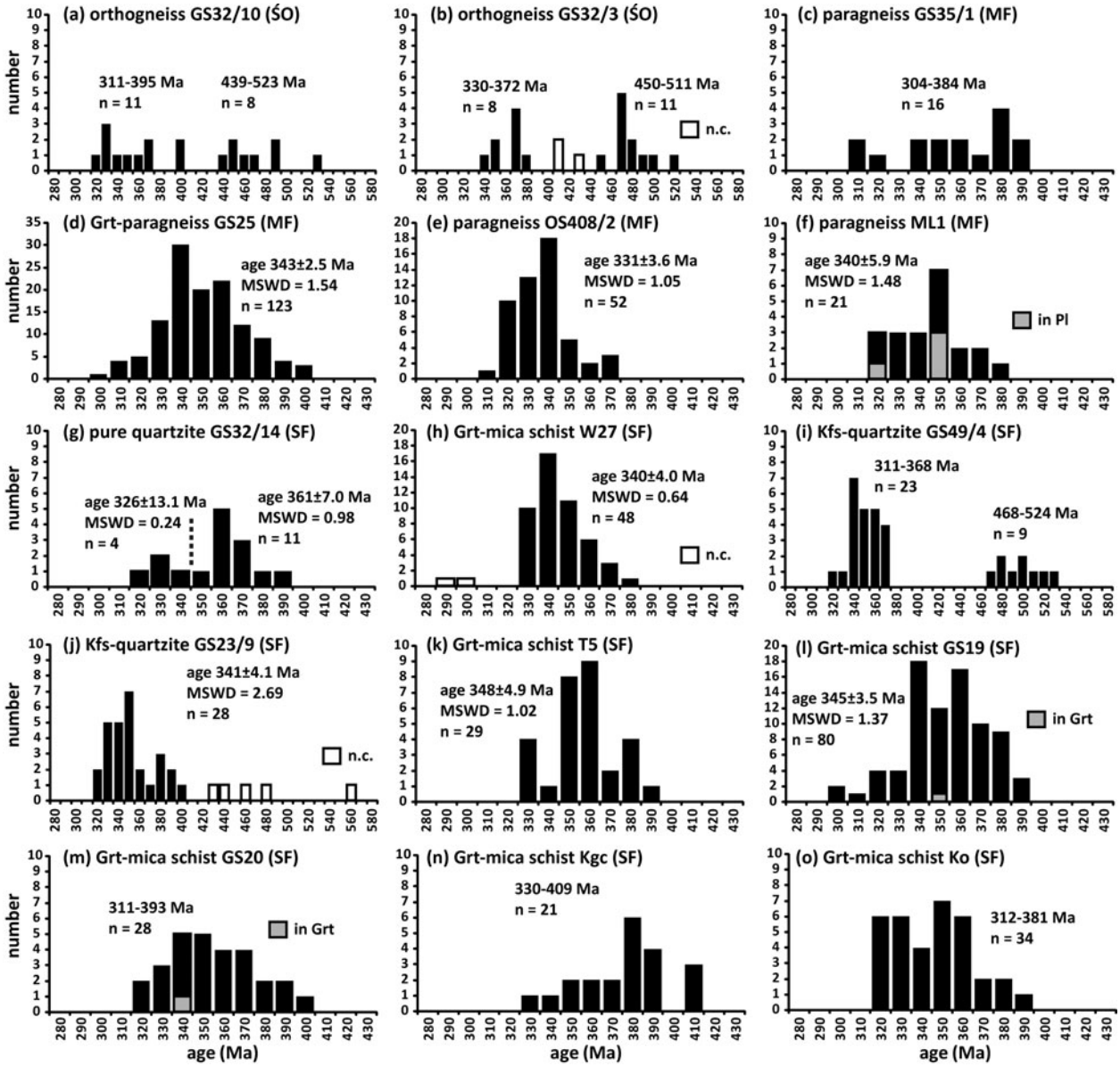

Figure 7. Results of the Th–U–total Pb monazite dating, which indicate *c*. 439–523 Ma monazite ages in the orthogneisses (a, b) and quartzites (i, j) and nearly continuous monazite growth during at least two metamorphic episodes at *c*. 330–340 Ma and *c*. 360–370 Ma. The calculated weighted average ages are listed with ±2σ error (95 % confidence level); n.c. – white bars not considered in the date ranges or in the calculation of the weighted average ages. ŚO – Śnieżnik orthogneisses, MF – Młynowiec Formation, SF – Stronie Formation.

The monazite in the paragneiss OS408/2 comprises subhedral to anhedral, 20–40 μm grains in matrix, which are homogeneous in high-contrast BSE imaging. Occasional 100–150 μm monazite grains are heterogeneous, demonstrating core–rim relations (Fig. 6f, g) or patchy zoning. The Th–U–total Pb geochronology revealed dates from 303 to 370 Ma, with a primary spectrum of 320–340 Ma and a weighted average age of 331 ± 3.6 Ma (2σ, $n = 52$, MSWD = 1.05; Fig. 7e).

The monazite in the paragneiss ML1 comprises subhedral to anhedral grains 20–80 μm across and present in the S2 matrix foliation (Fig. 6h) or as inclusions, which form the S1 foliation in albite (Fig. 6i) or oligoclase. Analyses of 17 grains provided dates from 312 to 377 Ma, with a weighted average age of 340 ± 5.9 Ma (2σ, $n = 21$, MSWD = 1.48; Fig. 7f). The monazite inclusions in plagioclases yielded four dates of ~317, ~345, ~347 and ~353 Ma.

5.c. Stronie Formation

The monazite in the quartzite GS32/14 comprises euhedral and anhedral grains that are 10–45 μm across in the rock matrix and are associated with muscovite or quartz. These monazite grains reflect growth (Fig. 6j) or patchy zoning (Fig. 6k) and commonly show porosity, which prevents EMP analyses. Analyses from nine grains provided a weighted average age of 361 ± 7.0 Ma (2σ, $n = 11$, MSWD = 0.98; Fig. 7g). One euhedral and two anhedral grains yielded younger

https://doi.org/10.1017/S0016756817000887 Published online by Cambridge University Press

ages with a weighted average of 326 ± 13.1 Ma (2σ, $n = 4$, MSWD = 0.24).

Anhedral and rare subhedral grains of monazite in the paragneiss W27 are 10–40 μm across and homogeneous in high-contrast BSE imaging (Fig. 6l). The monazite forms matrix grains that are associated with micas, quartz or feldspars. Occasionally, monazite forms inclusions in muscovite. The monazite dating provided 322–370 Ma single spot dates with a distinct weighted mean age domain at 340 ± 4.0 Ma (2σ, $n = 48$, MSWD = 0.64; Fig. 7h). Two small monazite grains yielded younger single spot dates of ~299 and ~284 Ma.

The monazite in the K-feldspar-bearing quartzite GS49/4 is present in the matrix or occasionally forms inclusions in muscovite. The monazite grains, which are 10–100 μm across, are subhedral to anhedral and exhibit porosity that is related to partial dissolution. The large grains (50–100 μm) exhibit patchy zoning or distinct cores and rims (Fig. 6m). Ten grains that were selected for geochronology yielded two age populations. The older population includes dates from 468 to 524 Ma with a weighted mean age of 488 ± 7.4 Ma (2σ, $n = 9$, MSWD = 2.69; Fig. 7i). The younger population includes dates from 311 to 368 Ma with a weighted mean age of 344 ± 2.8 Ma (2σ, $n = 23$, MSWD = 4.00). Large grains preserved records of older dates in dark patches and younger dates in bright patches, presumably from the re-equilibration of monazite during the Variscan event. Smaller, subhedral grains that show no alterations yielded Variscan ages of 336–352 Ma, indicating growth during the last metamorphic event (Fig. 6n). Distinct differences in composition between the older and younger population are expressed by 2.26–4.03 wt% vs 0.60–1.93 wt% Y_2O_3, <0.08 vs up to 0.18 wt% Eu_2O_3 and <0.04 vs up to 2.20 wt% SrO. The higher Eu and Sr contents in the younger domains most likely are related to the supply of these elements because of the breakdown of feldspars during quartzite formation.

The monazite in the K-feldspar-bearing quartzite GS32/9 comprises 10–80 μm, anhedral or rarely euhedral grains in the matrix (Fig. 6o). Two 10–20 μm grains yielded ~474 Ma and ~555 Ma dates. Older dates of ~427, ~436 and ~454 Ma were also obtained in the cores of 70–80 μm grains. The predominant younger age spectrum from 8 grains ranges from 318 to 393 Ma, with a weighted mean age of 341 ± 4.1 Ma (2σ, $n = 28$, MSWD = 2.69; Fig. 7j). Similarly to the quartzite GS49/4, the monazite shows compositional differences between the older and younger populations, such as 1.51–3.33 vs 0.18–1.30 wt% Y_2O_3 (supplementary Fig. S1j in Appendix III), <0.08 vs up to 0.26 wt% Eu_2O_3 (supplementary Fig. S2j in Appendix IV) and <0.17 vs up to 0.08–1.17 wt% SrO. The increase in Eu and Sr contents in the younger population is interpreted to be related to the supply of these elements because of the breakdown of feldspars.

Anhedral grains of monazite in the mica schist T5, which are 20–150 μm across, are heterogeneous in high-contrast BSE imaging and occur in the matrix (Fig. 6p). Analyses of 17 grains provided a weighted mean age of 348 ± 4.9 Ma (2σ, $n = 29$, MSWD = 1.02) with predominant dates of 340–360 Ma (Fig. 7k). Some analyses suggested minor age domains at ~330 and ~380 Ma. An increasing trend in Y (from 1.15–1.68 to 2.71–3.54 wt% Y_2O_3) (supplementary Fig. S1j in Appendix III) and decreasing trend in Eu (from 0.26–0.38 to 0.13–0.26 wt% Eu_2O_3) (supplementary Fig. S2j in Appendix IV) existed from older to younger monazite domains, which suggests that younger monazite growth was accompanied by or postdated the partial breakdown of garnet (releasing Y) and the crystallization of feldspars (accumulating Eu).

The monazite in the porphyroblastic garnet mica schist GS19 is highly abundant and forms anhedral grains that are homogeneous in high-contrast BSE imaging and 10–40 μm across (Fig. 6q, r). Matrix grains are predominant, although one monazite inclusion in garnet was also found. The Th–U–total Pb dating of 45 grains in two thin sections of the mica schist (GS19/2a and GS19/2b) provided a continuous spectrum from 330 to 380 Ma, with several younger dates at 293–330 Ma. The weighted average age is 345 ± 3.5 Ma (2σ, $n = 80$, MSWD = 1.37; Fig. 7l). The age histogram suggests two age domains at 330–340 and ~360 Ma, but these domains are not supported by structural data. One analysis of the monazite inclusion in garnet (Mnza6; Appendix II) yielded a date of 342 ± 44 Ma (2σ).

The monazite in the porphyroblastic garnet mica schist GS20 comprises 10–30 μm (rarely 50–80 μm) anhedral grains that are homogeneous or occasionally exhibit patchy zoning (Fig. 6s). All the analysed grains are present in the matrix, except for one monazite inclusion in garnet (Mnz11; Fig. 6t). Monazite dating provided a continuous spectrum of Th–U–total Pb dates from 311 to 393 Ma, with a weighted mean age of 349 ± 5.0 Ma (2σ, $n = 28$, MSWD = 2.24; Fig. 7m). The monazite Mnz11 in garnet yielded a ~333 Ma date. Geochronological data indicated prolonged monazite growth during potentially several events.

The monazite in the porphyroblastic garnet mica schist Kgc is present only as grain aggregates that are associated with quartz, plagioclase, muscovite, biotite and occasional remnants of altered allanite. The boundaries of these aggregates imitate the shape of the former phase, indicating a secondary origin of monazite that replaced allanite (Fig. 6u). The monazite exhibits dates from 330 to 409 Ma with a distinct age domain at 370–380 Ma (Fig. 7n). The weighted mean of the population is 371 ± 8.4 Ma (2σ, $n = 21$, MSWD = 1.67).

The monazite in the porphyroblastic garnet mica schist Ko comprises subhedral to anhedral grains with a size of 10–20 μm (Fig. 6v). Monazite is present in the matrix or forms common inclusions in muscovite or, less commonly, in chloritized biotite or quartz. The monazite geochronology revealed a continuous

https://doi.org/10.1017/S0016756817000887 Published online by Cambridge University Press

spectrum of dates from 312 to 381 Ma, with roughly pronounced age domains at 350–360 and 320–330 Ma. The weighted mean of the population is 338 ± 4.5 Ma (2σ, $n = 34$, MSWD = 1.93, Fig. 7o).

6. Discussion

6.a. Nature and significance of the Pre-Variscan, Early Palaeozoic thermal event

New monazite Th–U–total Pb dating has indicated the relatively weakly preserved record of the Early Palaeozoic thermal event in the strongly deformed metamorphic rocks of the OSD. Importantly, this record was obtained only in the metagranites and K-feldspar-bearing quartzites, whereas the paragneisses, pure quartzites and mica schists showed exclusively Variscan monazite ages (Table 2). The similar composition of the inherited Early Palaeozoic monazite domains, which are depleted in Eu and Sr (preferentially incorporated by feldspars) and show high Y and Th contents, suggests crystallization from a source with a granitic composition (cf. Williams *et al.* 2006). These results imply an inherited record of the Early Palaeozoic igneous event. Consequently, the presence of the Early Palaeozoic monazite age record is more likely related to specific origin of the K-feldspar quartzites and orthogneisses, and presumably does not indicate the metamorphism at this time.

Also, the directly contacting rocks of the MSG group do not indicate an influence of a pluton: there is no correlation between the monazite content and age, and the distance from the contact of the orthogneisses with the metasupracrustal rocks (Fig. 6; Table 2). The samples of K-feldspar-bearing quartzites (GS49/4 and GS23/9), interpreted to be enriched in volcaniclastic material (Jastrzębski, Budzyń & Stawikowski, 2016), were collected ∼90 m from this lithological contact (Fig. 2; Table 2). Four other samples of the MSG rocks represent a shorter distance from the metaigneous/meta-supracrustal rocks contact and provided Late Palaeozoic Th–U–total Pb ages, but no record of the earlier event(s). Lack of evidence of the contact metamorphism of the (meta)sedimentary rocks, which could have been induced by the emplacement of granitic magmas, possibly reflects the greater original distance between the supracrustal rocks and the Early Palaeozoic granites before the Variscan deformations. Thus, there is no documented reason to infer that the orthogneissic precursors intruded into the MSG supracrustal rocks, although certainly, in view of the existing geochemical data (Borkowska *et al.* 1990) and equivocal premises based on field observations (Don, 1964), such a possibility cannot be entirely excluded. As this eventuality is not confirmed by mineral assemblages and monazite geochronology, it cannot, however, be the fundament for the model construction.

Furthermore, a second possibility that the Cambro-Ordovician monazite ages reflect Early Palaeozoic regional metamorphism of the OSD metasupracrustal rocks was also not supported by the data collected in this study. The low-pressure – high-temperature (LP-HT) Cambro-Ordovician metamorphism in the Neoproterozoic rocks of the Tepla-Barrandian (Bohemian) unit (Fig. 1b) led to garnet formation, which was preserved in cores of two-stage garnet porphyroblasts (Peřestý *et al.*, 2017*a, b*). These authors correlated the Early Palaeozoic metamorphism with the rift-related, high geothermal gradient that was induced by the extension of North Gondwana and the formation of the passive margin of the opening Rheic Ocean. A similar tectonothermal setting that produced the Cambro-Ordovician LP-HT extensional fabric was also proposed for the amphibolite-rich Staré Město Belt, which is located along the eastern flank of the studied OSD unit (Štipská *et al.* 2001; Lexa *et al.* 2005). However, in the present study no evidence of multi-stage garnets has been observed, either in the Młynowiec–Stronie Group or the contacting Śnieżnik orthogneisses. This conclusion matches previous petrological and geochronological studies, which indicated that the growth of garnet in the OSD rocks occurred during the Variscan (tectono)thermal event(s) (e.g. Murtezi, 2006; Anczkiewicz *et al.* 2007; Jastrzębski, 2009; Skrzypek *et al.* 2011).

The K-feldspar quartzites were previously interpreted as tuffitic in origin (Smulikowski, 1979), which best explains the presence of the pre-Variscan, high Y and Th monazite grains in these rocks. More recently, the light quartzites in the OSD were proposed to be originated from quartz sands intercalated by pelitic rocks with an occasional admixture of tuffitic material, as evidenced by pre-tectonic feldspars and ∼490 Ma monazites (Jastrzębski, Budzyń & Stawikowski, 2016). The Stronie Formation includes various-scale bodies of felsic metavolcanites and metatuffites (e.g. Wojciechowska, 1972; Wojciechowska, Ziółkowska-Kozdrój & Gunia, 2001; Murtezi, 2006) with ∼490–500 Ma protolith ages (e.g. Murtezi & Fanning, 2005; Jastrzębski *et al.* 2015; Mazur *et al.* 2015). A local input of felsic volcanogenic material into the light quartzites in the Stronie Basin (Fig. 8a) could have been responsible for the inheritance of only the Early Palaeozoic monazites that were originally abundant and/or large enough to preserve their original composition during the Variscan recrystallization and metamorphism. Lack of possibly finer-grained detrital monazites recording Neoproterozoic and older components expected in the precursors of the MSG rocks could be interpreted as related to fluid-mediated processes during the Variscan overprint (Fig. 7). Despite the high diffusional closure temperature of monazite (above 800–900 °C; Cherniak *et al.* 2004; Gardes *et al.* 2006), a fluid-aided coupled dissolution–reprecipitation process has been experimentally demonstrated to be responsible for the compositional alteration of monazite with partial to complete Pb loss and the subsequent significant disturbance of the Th–U–Pb system (e.g. Williams *et al.* 2011; Budzyń, Konečný & Kozub-Budzyń,

https://doi.org/10.1017/S0016756817000887 Published online by Cambridge University Press

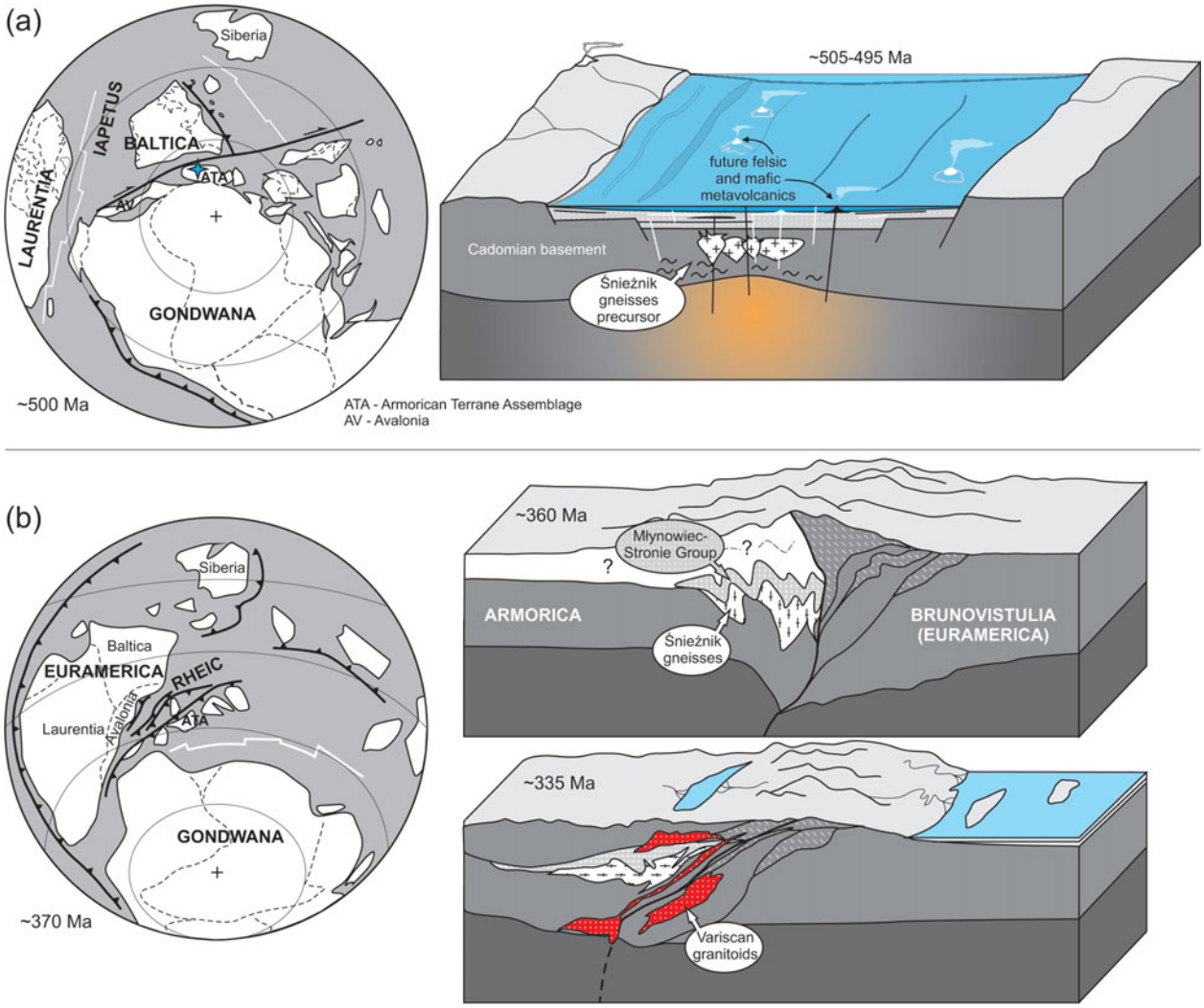

Figure 8. (Colour online) Cartoon model illustrating the evolution of (a) the Cambro-Ordovician and (b) the Devono-Carboniferous development of the present NE edge of the Bohemian Massif. The global reconstructions at ~500 Ma and 370 Ma were simplified and modified after Cocks & Torsvik (2006). Block diagrams not to scale.

2015; Budzyń *et al.* 2017). For this reason, the presence of scattered individual dates between 480 and 400 Ma in the Kfs-bearing quartzite GS23/9 (Fig. 7b, j) is interpreted to be related to partial Pb loss because of the fluid-mediated age disturbance of the Th–U–Pb system in the inherited Cambrian to Ordovician monazite domains mainly during younger, Variscan event(s).

Similarly, the Early Palaeozoic monazite-forming event was recorded in the Śnieżnik orthogneisses (samples GS32/10 and GS32/3; Fig. 7; Table 2). The low abundance of high Y and Th monazites prevented us from obtaining a broader dataset and tightly constraining the age of the protolith. Furthermore, the relatively wide range of monazite dates from ~439 to ~523 Ma without a distinct age domain suggests partial Pb loss that may have occurred because of a fluid-aided coupled dissolution–reprecipitation process during the younger Variscan event. The inner portions of the monazites preserved their original structure and chemical composition during the Variscan metamorphism, but the U–Pb zircon dating provided a more precise 495–510 Ma age for the granitic protoliths of the OSD's orthogneisses (e.g. Turniak, Mazur & Wysoczanski, 2000; Kröner *et al.* 2001).

In conclusion, we found that the Early Palaeozoic monazite ages recorded by the orthogneisses and MSG quartzites of volcano-detrital origin can be correlated with the timing of formation of their protoliths. It is proposed that the deposition of the light quartzites in the MSG reflects the onset of the ~490–500 Ma volcanic activity, which was followed by the deposition of pelites, carbonates and bimodal volcanism in the upper portions of the sedimentary basin (Fig. 8a). The Cambro-Ordovician timing of the deposition of the basal portions of the Stronie Formation implies not only a temporal but also a geochemical relationship between the syndepositional felsic volcanism and the voluminous granitic intrusions (e.g. Kröner *et al.* 2001; Wojciechowska, Ziółkowska-Kozdrój & Gunia, 2001; Murtezi, 2006) (Fig. 8a). These felsic plutonic rocks could be emplaced as crust-seated granites within the Cadomian basement. Their effusive and extrusive equivalents

https://doi.org/10.1017/S0016756817000887 Published online by Cambridge University Press

were concurrently formed in shallow-marine environments (Fig. 8a). In consequence, the crustal level difference between the zone of the pluton emplacement and the extrusive/effusive rocks can be expected. Detrital zircon age spectra of the OSD metasediments and inherited zircon ages in orthogneisses cluster at 540–660 Ma and 1.8–2.6 Ga (e.g. Turniak, Mazur & Wysoczanski, 2000; Żelaźniewicz *et al.* 2006; Jastrzębski *et al.* 2010; Mazur *et al.* 2012). This points to the affinity of the yet-to-be-determined basement on which the volcano-sedimentary MSG was deposited and into which the granites were intruded, to the Cadomian-age rocks known from the western part of the Saxothuringian zone (e.g. Linnemann *et al.* 2014). It cannot be excluded that the Wyszki paragneisses from the western part of the OSD (Mazur *et al.* 2015) or the Wądroże Wielkie orthogneisses located north of the Góry Sowie Block (Żelaźniewicz *et al.* 2004) are the nearest known equivalents of this Cadomian basement.

6.b. Timing and conditions of Variscan metamorphism and the significance of the lithological boundaries within the Variscan collisional zone

Structural observations (Fig. 5) and thermodynamic modelling (Fig. 4) suggest that both the orthogneisses and metavolcano-sedimentary rocks in their boundary zone underwent comparable metamorphic histories. The similar *P–T* records and parallel orientation of the deformational fabrics suggested that the contact between the meta-supracrustal rocks and orthogneisses did not reveal their large-scale tectonic juxtaposition, at least in terms of different crustal depths that were recorded by the contacting units prior to their recent mutual position. The results of the microstructural observations and thermodynamic modelling indicate that the penetrative metamorphic foliation in the paragneisses of the Młynowiec Formation and the Śnieżnik orthogneisses in the Żmijowiec–Średniak area developed under the same peak conditions, i.e. ~590–600 °C and 7–8 kbar (Fig. 4g, h). These *P–T* values correspond to the conditions previously calculated by Štipská *et al.* (2012) for mica schists from the Stronie Formation in the Mount Żmijowiec area (Fig. 5b). Although some calculations from the albite formation event (S1 planes) in the MSG amphibolites indicated a wider range of pressures from 4.5 to 10 kbar at temperatures of 460–550 °C (Fig. 4i), no other signs of high(er)-pressure metamorphism were present in the studied sector of the OSD. Our study indicates that the transition from S1- to S2-fabric formation (Jastrzębski *et al.* 2014, this study) was related to the thermal progression of regional metamorphism from greenschist- to amphibolite-facies metamorphism. Albite and its mineral inclusions are presumably typical greenschist-facies phases in the orthogneisses, paragneisses and amphibolites from the studied area of the OSD. In these rocks, the thermal progression to amphibolite-facies metamorphism was documented by the growth of oligoclase rims around the plagioclase blasts. Additionally, the S1–S2 relationships in garnet-bearing mica schists and paragneisses indicated that garnet growth was usually correlated with the transition from S1- to S2-fabric formation (including the studied samples from the Młynowiec Formation: ML1 and GS25) (Fig. 4c, d). In the paragneiss sample GS25, the transition from S1- to S2-fabric formation was reflected by an increase in pressure and temperature from 525 °C and 7 kbar to 590 °C and 8.2 kbar (Fig. 4h). The penetrative foliation in the mica schists from the Stronie Formation (including the dated samples Kgc, GS19, GS20, W27, and Ko) is invariably defined by the medium-pressure assemblage Qz–Ms–Bt–(Grt-rim) ± St Although the recently postulated early HP event in the Młynowiec–Stronie Group cannot be excluded (see Faryad & Kachlík, 2013; Twyrdy & Żelaźniewicz, 2017), we suggest that the S1-related Grt-rim mineral assemblages, namely, Grt(core)–Chl–Ctd in mica schists and Ms–Bt–Ab in paragneisses, reflect greenschist-facies conditions, which match earlier petrologic studies in the eastern part of the OSD (Smulikowski, 1979; Murtezi, 2006; Jastrzębski, Budzyń & Stawikowski, 2016).

Lithospheric-scale folding was recently proposed to explain the presence of both MP and (U?)HP rocks in the OSD (Štipská *et al.* 2012). Field observations indicated that the small eclogite bodies often have sharp, sometimes clearly tectonic contacts with the orthogneisses (e.g. Stawikowski, 2001, 2002), while geological mapping showed that eclogites or granulites generally did not outcrop within the Młynowiec–Stronie Group (e.g. Don, Skácel & Gotowała, 2003). Except for the volumetrically minor granulites and eclogites (e.g. Smulikowski, 1979; Bakun-Czubarow, 1992; Štípská, Schulmann & Kröner, 2004) (U?)HP metamorphic conditions were indicated for some of the orthogneisses in the closest vicinity of the eclogites (Bröcker & Klemd, 1996; Chopin *et al.* 2012*b*). Our new *P–T* estimations from the OSD orthogneisses indicate that the contact between the meta-supracrustal MSG rocks and the Śnieżnik orthogneisses, which is the main lithological boundary in the OSD, cannot be considered the main metamorphic boundary in this unit. Some of the OSD's orthogneisses have garnets with higher calcium content (e.g. Borkowska *et al.* 1990; Bröcker & Klemd, 1996; Stawikowski, 2006; Chopin *et al.* 2012*b*), which sometimes suggests the occurrence of (U)HP conditions (Bröcker & Klemd, 1996). Our thermodynamic modelling for these orthogneisses in the Śnieżnik–Żmijowiec area indicated that the interiors of the garnets with the Grs content of ~17 % were most likely equilibrated with biotite, muscovite and oligoclase, at 7.5 kbar and 600 °C (Table 1; Fig. 4). Neither HP relics nor the contrast between the *P–T* conditions for the orthogneisses and the adjacent metasupracrustal rocks were observed, so we infer that their precursors came into contact before the main stages of the Variscan tectonometamorphism.

https://doi.org/10.1017/S0016756817000887 Published online by Cambridge University Press

The geochronological results for the rocks that represent main lithologies of the OSD emphasize a prolonged Variscan metamorphic evolution. In recent tectonic models, the OSD has been considered a component of the Saxothuringia, which either collided with the Teplá–Barrandia and then docked to the Brunovistulia (Chopin *et al*. 2012*a*) or collided with the Brunovistulia and subsequently interacted with the Góry Sowie Block (Jastrzębski *et al*. 2014). Therefore, we can justify that the time extent of the metamorphism in the investigated section of the Variscan orogenic root was even more prolonged than previously considered. Our geochronological results indicated nearly continuous monazite growth from ∼400 to ∼300 Ma, although several samples provided records of two events at 360–370 Ma (GS32/3, GS32/14, Kgc; Fig. 7b, g, n) and 330–340 Ma (OS408/2, GS32/14, W27; Fig. 7e, g, h; Table 2). Distinguishing separate events in the broad age spectrum of 300–400 Ma in the remaining eight samples is disputable. The lack of structural premises regarding the monazite position in the rock fabrics and the relative compositional homogeneity of the monazite domains across the chronological range, including the very weak Y correlation with respect to garnet growth in garnet-bearing mica schists (sample T5, Appendix III), prevent us from directly defining separate events. However, the existence of weak domains in the age histograms of quartzites (Fig. 7g, j), garnet-bearing paragneiss (Fig. 7d) and mica schists (Fig. 7k, l, o), which match those mentioned above, suggests that monazite growth could have occurred during at least two separate tectonometamorphic events at ∼360 Ma and ∼340 Ma. The obtained results match the monazite geochronology study by Skrzypek *et al.* (2017), who confirmed a long duration for the monazite growth but considered ages of 360−340 Ma to represent the period of prograde monazite growth under amphibolite-facies conditions. In addition, our data correspond well with those from the rocks of the Staré Město Belt, which also experienced prolonged metamorphism from the progression of the Barrovian metamorphism at ∼368 Ma to the late, retrogressive metamorphic event at 340–330 Ma (Jastrzębski *et al.* 2013) (Fig. 8b). Our second age cluster also corresponds with the *c*. 340 Ma Variscan granitoids that were emplaced along the main OSD's tectonic boundaries (e.g. Štípská, Schulmann & Kröner, 2004; Oberc-Dziedzic, Kryza & Pin, 2015) (Fig. 8b). In conclusion, the Orlica–Śnieżnik Dome recorded two main, Late Devonian to Lower Carboniferous tectonometamorphic events respectively related to prograde part of the *P–T* path and the Visean granitoid magmatism connected with the uplift (Figs 1a, 8b).

The commonly small size of the monazite grains (<30 μm) in the studied rocks indicates that these grains could have been affected by fluid-mediated re-equilibration with the disturbance of the Th–U–Pb system, even under decreasing temperatures during retrogression. This observation may explain the wide age histograms and the presence of individual dates down to ∼300 Ma. These youngest ages may pinpoint the last exhumation stages of the OSD rocks, which were exposed to the infiltration of retrogressive fluids under subsurface conditions (Skrzypek *et al.* 2017). Although monazite was selected for this study because of this mineral's role as a powerful geochronological tool to provide records of igneous protoliths and younger metamorphic events, it has to be kept in mind that the stability of monazite may be affected by various post-growth processes.

7. Conclusions

In spite of premises that rifting of northern Gondwana and the opening of the Rheic Ocean in the Early Palaeozoic embraced collisional and/or metamorphic events, no monazite age evidence indicates that the metavolcano-sedimentary sequence (Młynowiec–Stronie Group) and its direct metagranitic surroundings in the Orlica–Śnieżnik Dome underwent a tectonometamorphic event(s) during that time. In addition, no petrologic evidence exists for an Early Palaeozoic thermal aureole along the margins of the metagranitic domains within the surrounding supracrustal rocks. The petrological and geochronological data collected in this study indicate that the protoliths of the studied part of MSG and the adjacent meta-igneous rocks mainly document the formation of the volcano-sedimentary basin and felsic intrusive and effusive/extrusive magmatism during the Cambro-Ordovician Gondwana break-up. Early Palaeozoic monazites, that record ∼490–500 Ma volcanic and plutonic events are rarely preserved in the both rock groups. They subsequently experienced the disturbance of the Th–U–Pb system during younger, Variscan events.

All the investigated rocks underwent prolonged and complex Variscan tectonometamorphic evolution resulted from the docking of the Gondwana-derived Armorican Terrane Assemblage to the Euramerica (Laurussia) continent. No large-scale tectonic juxtaposition of these two main lithostratigraphic units in the OSD is evident at their mutual contacts. On the contrary, a notable similarity exists in the *P–T–d–t* record of both rock types (with the amphibolite facies peak at 600–620°C). Together with the adjacent meta-supracrustal rocks, the studied orthogneisses indicate maximum burial depths that correspond to 7.5–8.0 kbar. No evidence of (U)HP metamorphism have been found in the studied rocks. The *P–T* data from both the metasediments and orthogneisses confirm that not the entire OSD represents the (U)HP unit, which must be considered in metamorphic maps and tectonic reconstructions of the Bohemian Massif. The interface between the meta-supracrustal rocks and the orthogneisses, the main lithological boundary, cannot be considered as the main metamorphic boundary in the OSD. Furthermore, our study suggests the long duration of the Variscan metamorphism that intensified at ∼360 and ∼340 Ma.

https://doi.org/10.1017/S0016756817000887 Published online by Cambridge University Press

Acknowledgements. This research was funded by the National Science Centre, Poland, grant number 2011/03/B/ST10/05638. Additionally, this study was supported by the INGPAN Research Funds (Project 'REE'). Lidia Jeżak and Piotr Dzierżanowski in Warsaw; Patrik Konečný, Ivan Holický and Viera Kollárová in Bratislava; and Gabriela Kozub-Budzyń in Kraków are gratefully acknowledged for their assistance with the electron microprobe analyses. We also thank Natalia Judkowiak for providing the rock sample N5BB and Józef Nowak for preparing all the thin sections. We are indebted to reviewers Jiří Žák and Ulf Linnemann for their helpful and constructive criticism. Most of the comments in the insightful review of the earlier version of this paper by Michael Bröcker were considered and helped to sharpen the presentation. We sincerely thank Mark Allen and Chad Deering for editorial assistance.

The authors want to express their deepest gratitude for the scientific achievements of Professor Jerzy Don, the unquestioned expert on the geological history of the Śnieżnik Massif, who passed away in November 2016. His numerous works and studies were the inspiration for us and served as indispensable, highly valuable background for our studies of the tectonometamorphism in the Orlica Śnieżnik Dome.

Supplementary material

To view supplementary material for this article, please visit https://doi.org/10.1017/S0016756817000887

References

Anczkiewicz, R., Szczepański, J., Mazur, S., Storey, C., Crowley, Q., Villa, I. M., Thirlwall, M. F. & Jeffries, T. E. 2007. Lu-Hf geochronology and trace element distribution in garnet: implications for uplift and exhumation of ultra-high pressure granulites in the Sudetes, SW Poland. *Lithos* **95**, 363–80.

Bakun-Czubarow, N. 1992. Quartz pseudomorphs after coesite and quartz exsolutions in eclogitic clinopyroxenes of the Złote Mountains in the Sudetes (SW Poland). *Archiwum Mineralogiczne* **48**, 3–25.

Bakun-Czubarow, N. 1998. Ilmenite-bearing eclogites of the West Sudetes – their geochemistry and mineral chemistry. *Archiwum Mineralogiczne* **51**, 29–110.

Bakun-Czubarow, N. 2001. Variscan UHP rock series of the Orlica-Śnieżnik Dome in the Sudetes compared with the other (U)HP rocks of the Bohemian Massif. *Abstracts of Sixth International Eclogite Conference, 2001 Shikoku, Japan*, 5–6.

Borkowska, M., Choukroune, P., Hameurt, J. & Martineau, F. 1990. A geochemical investigation of age, significance and structural evolution of the Caledonian-Variscan granite-gneisses of the Śnieżnik metamorphic area (central Sudetes, Poland). *Geologia Sudetica* **25**, 1–27.

Bröcker, M. & Klemd, R. 1996. Ultrahigh-pressure metamorphism in the Snieznik Mountains (Sudetes, Poland): P–T constraints and geological implications. *The Journal of Geology* **104**, 417–33.

Bröcker, M., Klemd, R., Cosca, M., Brock, W., Larionov, A. N. & Rodionov, N. 2009. The timing of eclogite-facies metamorphism and migmatization in the Orlica-Śnieżnik complex, Bohemian Massif: constraints from a geochronological multi-method study. *Journal of Metamorphic Geology* **27**, 385–403.

Bröcker, M., Klemd, R., Kooijman, E., Berndt, J. & Larionov, A. 2010. Zircon geochronology and trace element characteristics of eclogites and granulites from the Orlica-Śnieżnik complex, Bohemian Massif. *Geological Magazine* **147**, 339–62.

Brueckner, H. K., Medaris, L.G. & Bakun-Czubarow, N. 1991. Nd and Sr age and isotope patterns from Variscan eclogites of the eastern Bohemian Massif. *Neues Jahrbuch für Mineralogie, Abhandlungen* **163**, 169–96.

Budzyń, B., Harlov, D. E., Kozub-Budzyń, G. A. & Majka, J. 2017. Experimental constraints on the relative stabilities of the two systems monazite-(Ce) - allanite-(Ce) - fluorapatite and xenotime-(Y) - (Y,HREE)-rich epidote - (Y,HREE)-rich fluorapatite, in high Ca and Na-Ca environments under P-T conditions of 200–1000 MPa and 450–750 °C. *Mineralogy and Petrology*, **111**, 183–217.

Budzyń, B. & Jastrzębski, M. 2015. Monazite stability and the maintenance of Th-U-total Pb ages during post-magmatic processes in granitoids and host metasedimentary rocks: a case study from the Sudetes (SW Poland). *Geological Quarterly* **60**, 106–23.

Budzyń, B., Jastrzębski, M., Kozub-Budzyń, G. A. & Konečný, P. 2015. Monazite Th-U-total Pb geochronology and P–T thermodynamic modeling in a revision of the HP–HT metamorphic record in granulites from Stary Gierałtów (NE Orlica-Śnieżnik Dome, SW Poland). *Geological Quarterly* **59**, 700–17.

Budzyń, B., Konečný, P. & Kozub-Budzyń, G. A. 2015. Stability of monazite and disturbance of the Th-U-Pb system under experimental conditions of 250–350 °C and 200–400 MPa. *Annales Societatis Geologorum Poloniae* **85**, 405–24.

Buriánek, D., Verner, K., Hanžl, P. & Krumlová, H. 2009. Ordovician metagranites and migmatites of the Svratka and Orlice-Sněžník Units, northeastern Bohemian Massif. *Journal of Geosciences* **54**(2), 181–200.

Cháb, J., Stránik, Z. & Eliáš, M., 2007. *Geologická mapa České republiky 1: 500 000*. Prague: Czech Geological Survey.

Cherniak, D. J., Watson, E. B., Grove, M. & Harrison, T. M. 2004. Pb diffusion in monazite: a combined RBS/SIMS study. *Geochimica et Cosmochimica Acta* **68**, 829–40.

Chopin, F., Schulmann, K., Skrzypek, E., Lehmann, J., Dujardin, J. R., Martelat, J. E., Lexa, O., Corsini, M., Edel, J. B., Štípská, P. & Pitra, P. 2012a. Crustal influx, indentation, ductile thinning and gravity redistribution in a continental wedge: building a Moldanubian mantled gneiss dome with underthrust Saxothuringian material (European Variscan belt). *Tectonics* **31**, TC1013.

Chopin, F., Schulmann, K., Štípská, P., Martelat, J. E., Pitra, P., Lexa, O. & Pétri, B. 2012b. Microstructural and metamorphic evolution of a high pressure granitic orthogneiss during continental subduction (Orlica–Śnieżnik dome, Bohemian Massif). *Journal of Metamorphic Geology* **30**, 347–76.

Cocks, L. R. M. & Torsvik, T. H. 2006. European geography in a global context from the Vendian to the end of the Palaeozoic. In *European Lithosphere Dynamics*. (eds D. G. Gee & R. A. Stephenson), pp. 83–95. Geological Society of London, Memoir no. 32.

Cymerman, Z. 1992. Rotational ductile deformations in the Śnieżnik Metamorphic Complex. *Geological Quarterly* **36**, 393–420.

Cymerman, Z. 1997. Structure, kinematics and an evolution of the Orlica–Śnieżnik Dome, Sudetes. *Prace Państwowego Instytutu Geologicznego* **156**, 1–120.

Cymerman, Z., Piasecki, M. A. J. & Seston, R. 1997. Terranes and terrane boundaries in the Sudetes, northeast Bohemian Massif. *Geological Magazine* **134**, 717–25.

Don, J. 1964. Góry Złote i Krowiarki jako elementy składowe metamorfiku Śnieżnika [Góry Złote and Krowiarki as compositional elements of the Śnieżnik Metamorphic Unit]. *Geologia Sudetica* **1**, 79–117 (in Polish with extended English summary).

Don, J. 1982. Tektonika łupków strefy Siennej oraz korelacja rozwoju gnejsów z etapami deformacji metamorfiku Śnieżnika [The Sienna Synform and the relationship of genesis to the deformational stages distinguished in the Śnieżnik Metamorphic Massif (Sudetes)]. *Geologia Sudetica* **17**, 103–24 (in Polish with extended English summary).

Don, J., Dumicz, M., Wojciechowska, I. & Żelaźniewicz, A. 1990. Lithology and tectonics of the Orlica–Śnieżnik Dome, Sudetes – recent state of knowledge. *Neues Jahrbuch für Geologie und Paläontologie, Abhandlungen* **197**, 159–88.

Don, J., Skácel, J. & Gotowała, R. 2003. The boundary zone of the East and West Sudetes on the 1:50 000 scale geological map of the Velké Vrbno, Staré Město and Śnieżnik Metamorphic Units. *Geologia Sudetica* **35**, 25–59.

Drost, K., Linnemann, U., McNaughton, N., Fatka, O., Kraft, P., Gehmlich, M., Tonk, C. H. & Marek, J. 2004. New data on the Neoproterozoic-Cambrian geotectonic setting of the Teplá-Barrandian volcanosedimentary successions: geochemistry, U-Pb zircon ages, and provenance (Bohemian Massif, Czech Republic). *International Journal of Earth Sciences* **93**, 742–57.

Faryad, S. W. & Kachlík, V. 2013. New evidence of blueschist facies rocks and their geotectonic implication for Variscan suture(s) in the Bohemian Massif. *Journal of Metamorphic Geology* **31**, 63–82.

Fischer, G. 1936. Der Bau des Glatzer Schneegebirges. *Jahrbuch Preussischen Geologischen Landesanstalt* **56**, 712–32.

Franke, W. 2000. The mid-European segment of the Variscides: tectonostratigraphic units, terrane boundaries and plate tectonic evolution. In *Orogenic Processes, Quantification and Modelling in the Variscan Belt* (eds W. Franke, V. Haak, O Oncken & D. Tanner), pp. 35–61. Geological Society of London, Special Publication no. 179.

Franke, W. & Żelaźniewicz, A. 2000. The eastern termination of the Variscides: terrane correlation and kinematic evolution. In *Orogenic Processes: Quantification and Modelling in the Variscan Belt* (eds W. Franke, V. Haak, O. Oncken & D. Tanner), pp. 63–86. Geological Society of London, Special Publication no. 179.

Gardes, E., Jaoul, O., Montel, J., Seydoux-Guillaume, A. M. & Wirth, R. 2006. Pb diffusion in monazite: an experimental study of $Pb^{2+} + Th^{4+} \leftrightarrow 2Nd^{3+}$ interdiffusion. *Geochimica et Cosmochimica Acta* **70**, 2325–36.

Gordon, S. M., Schneider, D. A., Manecki, M. & Holm, D. K. 2005. Exhumation and metamorphism of an ultrahigh-grade terrane: geochronometric investigations of the Sudetes Mountains (Bohemia), Poland and Czech Republic. *Journal of the Geological Society, London* **162**, 841–55.

Gunia, T. 1990. Acritarcha i mikroproblematyki z wapieni krystalicznych okolicy Romanowa Górnego (Sudety Środkowe - Krowiarki) [Acritarcha and microproblematics of the crystalline limestones from the vicinity of Romanowo Górne (Central Sudetes - Krowiarki)]. *Geologia Sudetica* **24**, 101–37 (in Polish with English summary).

Holland, T. & Blundy, J. 1994. Non-ideal interactions in calcic amphiboles and their bearing on amphibole-plagioclase thermometry. *Contributions to Mineralogy and Petrology* **116**, 433–47.

Holland, T. J. B. & Powell, R. 1998. An internally consistent thermodynamic data set for phases of petrological interest. *Journal of Metamorphic Geology* **16**, 309–43.

Jastrzębski, M. 2009. A Variscan continental collision of the West Sudetes and the Brunovistulian terrane: a contribution from structural and metamorphic record of the Stronie Formation, the Orlica-Śnieżnik Dome, SW Poland. *International Journal of Earth Sciences* **98**, 1901–23.

Jastrzębski, M., Budzyń, B. & Stawikowski, W. 2016. Structural, metamorphic and geochronological record in the Goszów quartzites of the Orlica-Śnieżnik Dome (SW Poland): implications for the polyphase Variscan tectonometamorphism of the Saxothuringian Terrane. *Geological Journal* **51**, 455–79.

Jastrzębski, M., Stawikowski, W., Budzyń, B. & Orłowski, R. 2014. Migmatization and large-scale folding in the Orlica-Śnieżnik Dome, NE Bohemian Massif: Pressure-Temperature-time-deformation constraints on Variscan terrane assembly. *Tectonophysics* **630**, 54–74.

Jastrzębski, M., Żelaźniewicz, A., Majka, J., Murtezi, M., Bazarnik, J. & Kapitonov, I. 2013. Constraints on the Devonian–Carboniferous closure of the Rheic Ocean from a multi-method geochronology study of the Staré Město Belt in the Sudetes (Poland and the Czech Republic). *Lithos* **170–171**, 54–72.

Jastrzębski, M., Żelaźniewicz, A., Murtezi, M., Sergeev, S. & Larionov, A. N. 2015. The Moldanubian Thrust Zone – a terrane boundary in the Central European Variscides refined based on lithostratigraphy and U-Pb zircon geochronology. *Lithos* **220–223**, 116–32.

Jastrzębski, M., Żelaźniewicz, A., Nowak, I., Murtezi, M. & Larionov, A. N. 2010. Protolith age and provenance of metasedimentary rocks in Variscan allochthon units: U–Pb SHRIMP zircon data from the Orlica–Śnieżnik Dome, West Sudetes, *Geological Magazine* **147**, 416–33.

Klemd, R. & Bröcker, M. 1999. Fluid influence on mineral reactions in ultrahigh-pressure granulites: a case study in the Śnieżnik Mts. (West Sudetes, Poland). *Contributions to Mineralogy and Petrology* **135**, 358–73.

Konečný, P., Siman, P., Holický, I., Janák, M. & Kollárová, V. 2004. Method of monazite dating by means of the electron microprobe. *Mineralogia Slovaca*, **36**, 225–35 (in Slovak, with English abstract).

Kröner, A., Jaeckel, P., Hegner, E. & Opletal, M. 2001. Single zircon ages and whole-rock Nd isotopic systematic of early Paleozoic granitoid gneisses from the Czech and Polish Sudetes (Jizerske hory, Karkonosze Mountains and Orlica–Śnieżnik Complex). *International Journal of Earth Sciences* **90**, 304–24.

Kryza, R., Pin, C. & Vielzeuf, D. 1996. High-pressure granulites from the Sudetes (south-west Poland): evidence of crustal subduction and collision thickening in

the Variscan Belt. *Journal of Metamorphic Geology* **14**, 531–46.

Kusiak, M. A., Suzuki, K., Dunkley, D. J., Lekki, J., Bakun-Czubarow, N., Paszkowski, M. & Budzyń, B. 2008. EPMA and PIXE dating of monazite in granulites from Stary Gierałtów, NE Bohemian Massif, Poland. *Gondwana Research* **14**, 675–85.

Lange, U., Bröcker, M. & Armstrong, R. 2005a. Sm–Nd and U–Pb dating of high-pressure granulites from the Zlote and Rychleby Mts (Bohemian Massif, Poland and Czech Republic). *Journal of Metamorphic Geology* **23**, 133–45.

Lange, U., Bröcker, M., Armstrong, R., Żelaźniewicz, A., Trapp, E. & Mezger, K. 2005b. The orthogneisses of the Orlica-Śnieżnik complex (West Sudetes, Poland): geochemical characteristics, the importance of pre-Variscan migmatization and constraints on the cooling history. *Journal of the Geological Society, London* **162**, 973–84.

Lange, U., Bröcker, M., Mezger, K. & Don, J. 2002. Geochemistry and Rb-Sr geochronology of a ductile shear zone in the Orlica–Śnieżnik Dome (West Sudetes, Poland). *International Journal of Earth Sciences* **91**, 1005–16.

Lexa, O., Štípská, P., Schulmann, K., Baratoux, L. & Kröner, A. 2005. Contrasting textural record of two distinct metamorphic events of similar P-T conditions and different durations. *Journal of Metamorphic Geology* **23**, 649–66.

Linnemann, U., Gerdes, A., Hofmann, M. & Marko, L. 2014. The Cadomian Orogen: Neoproterozoic to Early Cambrian crustal growth and orogenic zoning along the periphery of the West African Craton – constraints from U–Pb zircon ages and Hf isotopes (Schwarzburg Antiform, Germany). *Precambrian Research* **244**, 236–78.

Linnemann, U., Pereira, F., Jeffries, T. E., Drost, K. & Gerdes, A. 2008. The Cadomian Orogeny of the Rheic Ocean: the diachrony of the geotectonic processes constrained by LA-ICP-MS U-Pb zircon dating (Ossa-Morena and Saxo-Thuringian Zones, Iberian and Bohemian Massifs). *Tectonophysics* **461**, 21–43.

Maluski, H., Rajlich, P. & Souček, J. 1995. Pre-Variscan, Variscan and early Alpine thermo-tectonic history of the north-eastern Bohemian Massif: $^{40}Ar/^{39}Ar$ study. *Geologische Rundschau* **84**, 345–58.

Matte, P., Maluski, P. H., Rajlich, P. & Franke, W. 1990. Terrane boundaries in the Bohemian Massif: result of large-scale Variscan shearing. *Tectonophysics* **177**, 151–70.

Mazur, S., Aleksandrowski, P., Kryza, R. & Oberc-Dziedzic, T. 2006. The Variscan Orogen in Poland. *Geological Quarterly* **50**, 89–118.

Mazur, S., Szczepański, J., Turniak, K. & McNaughton, N. J., 2012. Location of the Rheic suture in the eastern Bohemian Massif: evidence from detrital zircon data. *Terra Nova* **24**, 199–206.

Mazur, S., Turniak, L., Szczepański, J. & McNaughton, N. J. 2015. Vestiges of Saxothuringian crust in the Central Sudetes, Bohemian Massif: zircon evidence of a recycled subducted slab provenance. *Gondwana Research* **27**, 825–39.

Mikulski, S. Z., Williams, I. S. & Bagiński, B. 2013. Early Carboniferous (Viséan) emplacement of the collisional Kłodzko–Złoty Stok granitoids (Sudetes, SW Poland): constraints from geochemical data and zircon U–Pb ages. *International Journal of Earth Sciences* **102**,1007–27.

Montel, J. M., Foret, S., Veschambre, M., Nicollet, C. & Provost, A. 1996. Electron microprobe dating of monazite. *Chemical Geology* **131**, 37–53.

Murphy, J. B., Gutiérrez-Alonso, G., Nance, R. D., Fernández-Suárez, J., Keppie, J. D., Quesada, C., Strachan, R. A. & Dostal, J. 2006. Origin of the Rheic ocean: rifting along a Neoproterozoic suture? *Geology* **34**, 325–8.

Murtezi, M. 2006. The acid metavolcanic rocks of the Orlica–Śnieżnik Dome: their origin and tectono-metamorphic evolution. *Geologia Sudetica* **38**, 1–38.

Murtezi, M. & Fanning, M. 2005. Petrogenesis, age and tectono-metamorphic evolution of the acid metavolcanites of the Stronie Formation (Orlica-Śnieżnik Dome, Sudetes, SW Poland). *Geolines* **19**, 85.

Nance, R. D., Gutiérrez-Alonso, G., Keppie, J. D., Linnemann, U., Murphy, J. B., Quesada, C., Strachan, R. A. & Woodcock, N. H. 2012. A brief history of the Rheic Ocean. *Geoscience Frontiers* **3**, 125–35.

Oberc, J. 1965. Postępy geologii prekambru na Dolnym Śląsku [Advances in the Pre-Cambrian geology of Lower Silesia]. *Przegląd Geologiczny* **13**, 298–304 (in Polish with English abstract).

Oberc-Dziedzic, T., Kryza, R., Mochnacka, K. & Larionov, A. 2010. Ordovician passive continental margin magmatism in the Central-European Variscides: U-Pb zircon data from the SE part of the Karkonosze-Izera Massif, Sudetes, SW Poland. *International Journal of Earth Sciences* **99**, 27–46.

Oberc-Dziedzic, T., Kryza, R. & Pin, C. 2015. Variscan granitoids related to shear zones and faults: examples from the Central Sudetes (Bohemian Massif) and the Middle Odra Fault Zone. *International Journal of Earth Sciences* **104**, 1139–66.

Peřestý, V., Lexa, O., Holder, R., Jeřabek, P., Racek, M., Štípská, P., Schulmann, K. & Hacker, B. 2017a. Metamorphic inheritance of Rheic passive margin evolution and its early-Variscan overprint in the Teplá-Barrandian Unit, Bohemian Massif. *Journal of Metamorphic Geology* **35**, 327–55.

Peřestý, V., Lexa, O., Štípská, P., Jeřabek, P. & Racek, M. 2017b. Pre-Variscan rift-related structure and metamorphism in the Domažlice Crystalline Complex (the Teplá-Barrandian Domain, Bohemian Massif). *Acta Mineralogica-Petrographica* **32**, 31–2.

Petrík, I. & Konečný, P. 2009. Metasomatic replacement of inherited metamorphic monazite in a biotite-garnet granite from the Nízke Tatry Mountains, Western Carpathians, Slovakia: chemical dating and evidence for disequilibrium melting. *American Mineralogist* **94**, 957–74.

Pin, C., Kryza, R., Oberc-Dziedzic, T., Mazur, S., Turniak, K. & Waldhausrová, J. 2007. The diversity and geodynamic significance of Late Cambrian (ca. 500 Ma) felsic anorogenic magmatism in the northern part of the Bohemian Massif: a review based on Sm-Nd isotope and geochemical data. *Geological Society of America Special Paper* **423**, 209–29.

Pin, C. & Marini, F. 1993. Early Ordovician continental break-up in Variscan Europe: Nd–Sr isotope and trace element evidence from bimodal igneous associations of the Southern Massif Central, France. *Lithos* **29**, 177–96.

Redlińska-Marczyńska, A. & Żelaźniewicz, A. 2011. Gneisses in the Orlica-Śnieznik Dome, West Sudetes:

a single batholitic protolith or a more complex origin? *Acta Geologica Polonica* **61**, 307–39.

Redlińska-Marczyńska, A., Żelaźniewicz, A. & Fanning, C. M. 2016. An insight into a gneiss core of the Orlica-Śnieżnik Dome, NE Bohemian Massif: new structural and U–Pb zircon data. *Geological Quarterly* **60**, 714–36.

Sawicki, L. 1995. *Geological map of Lower Silesia with adjacent Czech and German territories 1:100 000*. Warsaw: Państwowy Instytut Geologiczny.

Schmidt, M. W. 1992. Amphibole composition in tonalite as a function of pressure: an experimental calibration of the Al-in-hornblende barometer. *Contributions to Mineralogy and Petrology* **110**, 304–10.

Schneider, D. A., Zahniser, S. J., Glascock, J. M., Gordon, S. M. & Manecki, M. 2006. Thermochronology of the West Sudetes (Bohemian Massif): rapid and repeated eduction in the eastern Variscides, Poland and Czech Republic. *American Journal of Science* **306**, 846–73.

Skrzypek, E., Bosse, V., Tetsuo Kawakami, T., Martelat, J. E. & Štípská, P. 2017. Transient allanite replacement and prograde to retrograde monazite (re)crystallization in medium-grade metasedimentary rocks from the Orlica-Śnieżnik Dome (Czech Republic/Poland): textural and geochronological arguments. *Chemical Geology* **449**, 41–57.

Skrzypek, E., Lehmann, J., Szczepański, J., Anczkiewicz, R., Štípská, P., Schulmann, K., Kröner, A. & Białek, D. 2014. Time-scale of deformation and intertectonic phases revealed by P-T-D-t relationships in the orogenic middle crust of the Orlica-Śnieżnik Dome, Polish/Czech Central Sudetes. *Journal of Metamorphic Geology* **32**, 981–1003.

Skrzypek, E., Štípská, P., Schulmann, K., Lexa, O. & Lexova, M. 2011. Prograde and retrograde metamorphic fabrics – a key for understanding burial and exhumation in orogen (Bohemian Massif). *Journal of Metamorphic Geology* **29**, 451–72.

Smulikowski, K. 1979. Ewolucja polimetamorficzna krystaliniku Śnieżnika Kłodzkiego i Gór Złotych w Sudetach [Polymetamorphic evolution of the Śnieżnik Kłodzki–Góry Złote Metamorphic Unit in the Sudetes.]. *Geologia Sudetica* **14**, 7–76 (in Polish with extended English summary).

Stawikowski, W. 2001. Strefy kontaktowe eklogitów i gnejsów w jednostkach Gierałtowa i Śnieżnika (kopuła orlicko-śnieżnicka) [Contact zones between eclogites and gneisses in the Gierałtów and Śnieżnik Units (Orlica-Śnieżnik-Dome)]. *Przegląd Geologiczny* **49**, 153–60 (in Polish with English abstract).

Stawikowski, W. 2002. Contacts between high-P eclogites and gneisses in the Lądek–Śnieżnik Metamorphic Unit, the West Sudetes. *GeoLines* **14**, 84–5.

Stawikowski, W. 2006. The problem of garnet composition in eclogite-bearing gneisses from the Śnieżnik Metamorphic Complex (Western Sudetes). *GeoLines* **20**, 122–3.

Steltenpohl, M. G., Cymerman, Z., Krogh, E. J. & Kunk, M. J. 1993. Exhumation of eclogitized continental basement during Variscan lithospheric delamination and gravitational collapse, Sudety Mountains, Poland. *Geology* **21**, 1111–4.

Štípská, P., Chopin, F., Skrzypek, E., Schulmann, K., Pitra, P., Lexa, O., Martelat, J. E., Bollinger, C. & Žáčková, E. 2012. The juxtaposition of eclogite and mid-crustal rocks in the Orlica–Śnieżnik Dome, Bohemian Massif. *Journal of Metamorphic Geology* **30**, 213–34.

Štípská, P., Schulmann, K. & Kröner, A. 2004. Vertical extrusion and middle crust spreading of omphacite granulite: a model of syn-convergent exhumation (Bohemian Massif, Czech Republic). *Journal of Metamorphic Geology* **22**, 179–98.

Štípská, P., Schulmann, K., Thompson, A. B., Ježek, J. & Kröner, A. 2001. Thermo-mechanical role of a Cambro-Ordovician paleorift during the Variscan collision: the NE margin of the Bohemian Massif. *Tectonophysics* **332**, 239–53.

Szczepański, J. & Ilnicki, S. 2014. From Cadomian arc to Ordovician passive margin: geochemical records preserved in metasedimentary successions of the Orlica-Śnieżnik Dome in SW Poland. *International Journal of Earth Sciences* **103**, 627–47.

Tait, J. A., Bachtadse, V., Franke, W. & Soffel, H. C. 1997. Geodynamic evolution of the European Variscan fold belt: palaeomagnetic and geological constraints. *Geologische Rundschau* **86**, 585–98.

Teisseyre, J. 1961. Skały wapienno-krzemianowe masywu Śnieżnika [The calc-silicate rocks of the Śnieżnik Mountains in the Sudetes]. *Archiwum Mineralogiczne* **23**, 155–96 (in Polish with English abstract).

Turniak, K., Mazur, S. & Wysoczanski, R. 2000. SHRIMP zircon geochronology and geochemistry of the Orlica-Śnieżnik gneisses (Variscan belt of Central Europe) and their tectonic implications. *Geodinamica Acta* **13**, 293–312.

Twyrdy, M. & Żelaźniewicz, A. 2017. Indications of HP events in the volcanosedimentary succession of the Orlica–Śnieżnik Dome, NE Bohemian Massif: data from a marble-amphibolite interface. *Geological Quarterly* **61**, 435–49.

von Raumer, J. F. & Stampfli, G. M. 2008. The birth of the Rheic Ocean – Early Palaeozoic subsidence patterns and subsequent tectonic plate scenarios. *Tectonophysics* **461**, 9–20.

von Raumer, J. F., Stampfli, G. M., Arenas, R. & Sánchez Martínez, S. 2015. Ediacaran to Cambrian oceanic rocks of the Gondwana margin and their tectonic interpretation. *International Journal of Earth Sciences* **104**, 1107–21.

Vozárová, A., Konečný, P., Šarinová, K. & Vozár, J. 2014. Ordovician and Cretaceous tectonothermal history of the Southern Gemericum Unit from microprobe monazite geochronology (Western Carpathians, Slovakia). *International Journal of Earth Sciences (Geologische Rundschau)* **103**, 1005–22.

Walczak, K. 2011. *Interpretacja datowań Sm-Nd i Lu-Hf granatów w skałach wysokociśnieniowych i wysokotemperaturowych w świetle badań dystrybucji pierwiastków śladowych* [*Interpretation of Sm-Nd and Lu-Hf dating of garnets in high-pressure and high-temperatures rocks in the light of REE distribution studies*]. Ph.D. thesis, Institute of Geological Sciences, Polish Academy of Sciences, Kraków. Published thesis (In Polish).

Whitney, D. L. & Evans, B. W. 2010. Abbreviations for names of rock-forming minerals. *American Mineralogist* **95**, 185–7.

Williams, M. L., Jercinovic, M. J., Goncalves, P. & Mahan, K. 2006. Format and philosophy for collecting, compiling, and reporting microprobe monazite ages. *Chemical Geology* **225**, 1–15.

Williams, M. L., Jercinovic, M. J. & Hetherington, C. J. 2007. Microprobe monazite geochronology: Understanding geologic processes by integrating composition and chronology. *Annual Review of Earth and Planetary Sciences* **35**, 135–175.

Williams, M. L., Jercinovic, M. J., Harlov, D. E., Budzyń, B. & Hetherington, C. J., 2011. Resetting monazite ages during fluid-related alteration. *Chemical Geology* **283**, 218–25.

Wojciechowska, I. 1972. Preliminary results of investigation on so-called "Quartzites" in the neighbourhood of Romanowo (Stronie Complex), NW part of Krowiarki (East Sudetes). *Bulletin of the Polish Academy of Sciences, Earth Sciences* **20**, 273–77.

Wojciechowska, I. 1993. Budowa geologiczna i tektonika Gór Złotych i Krowiarek jako tło rozwoju mineralizacji rudnej (Ziemia Kłodzka, Sudety) [Geological structure and tectonics of Góry Złote and Krowiarki as a background for development of ore mineralization (Ziemia Kłodzka, Sudety)]. *Prace Geologiczno-Mineralogiczne, Acta Univeritatis Wratislaviensis* **33**, 5–49 (in Polish with English abstract).

Wojciechowska, I., Ziółkowska-Kozdrój, M. & Gunia, P. 2001. Petrography and geochemistry of leptites from the Skrzynka Dislocation Zone (Eastern Sudetes, SW Poland) – preliminary results. *Bulletin of the Polish Academy of Sciences, Earth Sciences* **49**, 1–11.

Žák, J., Kraft, P. & Hajná, J. 2013. Timing, styles, and kinematics of Cambro-Ordovician extension in the Teplá–Barrandian Unit, Bohemian Massif, and its bearing on the opening of the Rheic Ocean. *International Journal of Earth Sciences* **102**, 415–33.

Żelaźniewicz, A. 1988. Orthogneisses due to irrotational extension, a case from the Sudetes, Bohemian massif. *Geologische Rundschau* **77**, 671–82.

Żelaźniewicz, A, Dörr, W., Bylina, P., Franke, W., Haack, U., Heinisch, H., Schastok, J., Grandmontagne, K. & Kulicki, C., 2004. The eastern continuation of the Cadomian orogen: U-Pb zircon evidence from Saxo-Thuringian granitoids in south-western Poland and the northern Czech Republic. *International Journal of Earth Sciences* **93**, 773–81.

Żelaźniewicz, A., Jastrzębski, M., Redlińska-Marczyńska, A. & Szczepański, J. 2014. The Orlica–Śnieżnik Dome, the Sudetes, in 2002 and 12 years later. *Geologia Sudetica* **42**, 105–23.

Żelaźniewicz, A., Nowak, I., Larionov, A. & Presnyakov, S. 2006. Syntectonic Lower Ordovician migmatite and post-tectonic Upper Viséan syenite in the western limb of the Orlica-Śnieżnik Dome, West Sudetes: U-Pb SHRIMP data from zircons. *Geologia Sudetica* **38**, 63–80.